MicroRNA-547-5p-mediated interleukin-33/suppressor of tumorigenicity 2 signaling underlies the genesis and maintenance of neuropathic pain and is targeted by the therapy with bone marrow stromal cells

Ju Zhou, Ting Zhuang, Peng Ma, Lidong Shan, Xiao-Dong Sun, Shan Gong, Jin Tao, Xian-Min Yu ⓘ and Xinghong Jiang

Abstract

Interleukin-33 (IL-33)/suppressor of tumorigenicity 2 (ST2) signaling is known to promote inflammation and the genesis and maintenance of neuropathic pain. However, it remained mostly unknown how IL-33/ST2 signaling can be enhanced by neuropathic stimulations. Here, we report that the chronic constriction nerve injury (CCI)-induced increases in the expression of IL-33 and ST2 and a decrease in microRNA (miRNA)-547-5p not only in the dorsal root ganglia (DRG) but also in spinal dorsal horn (SDH) ipsilateral to the CCI. We found that increasing endogenous miRNA-547-5p by the intrathecal (i.t.) infusion of agomir-miR-547-5p did not produce any effect in naive rats but blocked the CCI-induced increases in the IL-33 and ST2, and pain sensitivity. The reducing endogenous miRNA-547-5p by the i.t. delivering antagomir-miR-547-5p into naive rats caused significant changes in IL-33 and ST2 expressions in both the DRG and SDH, and pain sensitivity, which were similar to those induced by the CCI. Since increasing IL-33 by the i.t. infusion of recombinant IL-33 produced no change in the expression of miR-547-5p, and the CCI still reduced miR-547-5p expression in rats with the IL-33 knockdown, we conclude that the reduction of miR-547-5p can be an upstream event leading to the enhancement of IL-33/ST2 signaling induced by the CCI. The intravenous application of bone marrow stromal cells (BMSCs) reduced the depression of miR-547-5p in both the DRG and SDH, and pain hypersensitivity produced by the CCI or antagomir-miR547-5p application. However, the BMSC effect was significantly occluded by the pretreatment with miR-547-5p agomir or the IL-33 knockdown, demonstrating a novel mechanism underlying the BMSC therapy.

Keywords

MicroRNA, IL-33/ST2, neuropathic pain, stem cells, dorsal root ganglia, spinal cord, miRNA-547-5p, bone marrow stromal cells

Introduction

Understanding the mechanisms and developing more effective therapy of neuropathic pain are still challenges. Recent studies have shown that the interleukin-33 (IL-33)/suppressor of tumorigenicity 2 (ST2) signaling promotes inflammation[1–5] and plays critical roles in the development of neuropathic pain.[6–10] Great efforts have been made to clarify mechanisms that may be involved in the regulation of IL-33/ST2 signaling (see reviews: Fairlie-Clarke et al.,[4] Fattori et al.,[10]

Key Laboratory of Pain Basic Research and Clinical Therapy, Department of Physiology and Neurobiology, Medical College of Soochow University, Suzhou, China

Corresponding Authors:
Xian-Min Yu, Key Laboratory of Pain Basic Research and Clinical Therapy, Department of Physiology and Neurobiology, Medical College of Soochow University, Suzhou 215123, China.
Email: yuxianminyu1981@hotmail.com
Xinghong Jiang, Key Laboratory of Pain Basic Research and Clinical Therapy, Department of Physiology and Neurobiology, Medical College of Soochow University, Suzhou 215123, China.
Email: jiangxinghong@suda.edu.cn

Molofsky et al.[11]). MicroRNAs (miRNAs) have been found to be involved in the regulation of IL-33/ST2 signaling. For example, enhancing the expression of miRNA-487b not only inhibits the expression of IL-33 and ST2 but also improves the heart function.[12] The expression of IL-33 and ST2 is increased in allergic rhinitis patients, while miRNA-487b expression reduced. The upregulation of miRNA-487b reduces the immunoglobulin E, proinflammatory cytokines, and the mitigation of pathological alterations.[13] Interestingly, IL-33/ST2 may promote gut mucosal healing through increasing the expression of miRNA-320 in colitic mice during the recovery period, which facilitates the epithelial restitution and the inflammation resolution.[14]

Recently, it has been documented that neuropathic pain induced by nerve injury can be relieved by delivering bone marrow stromal cells (BMSCs) locally, intrathecally, or systematically (see reviews: Fortino et al.,[15] Huh et al.,[16] Han et al.[17]). However, detailed mechanisms underlying the genesis and maintenance of neuropathic pain, as well as its stem cell-based therapeutic intervention remained not entirely clear. To address these issues, we conducted this research in which we identified that via depressing miRNA-547-5p, the constriction nerve injury (CCI) induced the enhancement of IL-33/ST2 signaling in both the dorsal root ganglia (DRG) and spinal dorsal horn (SDH), and pain sensitivity, and that via blocking the miRNA-547-5p-mediated IL-33/ST2 signaling, BMSCs reduced the CCI-induced pain hypersensitivity.

Materials and methods

Animals

A total of 332 adult Sprague-Dawley rats (male, 180–200 g; SLAC Laboratory Animal, Shanghai, China) were used for this study. The animals were housed on a 12-hr light/dark cycle with free access to food and water. Before any experiments, rats were adapted to the testing environment for three days.

All animal experiments were performed following the guidelines of the Animal Care and Use Committee of the Medical College of Soochow University and approved by the Ethics Committee of Soochow University (AP# SUDA20200316A02) according to the ethical standards of the International Association for the Study of Pain.

Surgery procedures

For creating a CCI model, rats were deeply anesthetized with intraperitoneal (i.p.) injection of 4% chloral hydrate. The right sciatic nerve and its three terminal branches—the sural, common peroneal, and tibial nerves—were exposed by sectioning through the biceps femoris. Care was taken not to touch or stretch the spared sural nerve. The common peroneal and tibial nerves were loosely ligated with 6.0 silk until the shot flick of the ipsilateral hind limb was observed. The muscle and skin were then closed in two separate layers. For the sham surgeries, the nerves were exposed as described above without ligation. Lidocaine (2%, Sihuan Pharmaceutical, Beijing, China) was locally applied on the surgical region to reduce pain. After the CCI or sham operation, rats were allocated in individual cages with food and water and carefully observed until completely recovered from anesthesia. No adverse event such as paradoxical excitement or vomiting was found after the i.p. injection of 4% chloral hydrate.

Behavioral analysis

Mechanical withdrawal threshold (MWT) and thermal withdrawal latency (TWL) of rats' hind paw were measured between 9 and 12 am as described previously.[18,19] In brief, for MWT tests, rats were placed in an individual transparent chamber on a metal mesh table for 30 min and then tested with calibrated Von Frey filaments, ranging from 0.4 to 26 g (Stoelting, Wood Dale, IL, USA). The filaments were applied perpendicularly to the plantar surface of rats. Each test was for 5 s. Withdrawal of the tested hind paw was considered as a positive response. The pattern of negative and positive responses was converted to the MWT according to the formula: 50% threshold (g) $= (10[Xf + K\delta])/10,000$ (Xf: the final bending force of the Von Frey filament; K: the tabular value for the pattern of positive/negative responses; δ: 0.22).

Thermal stimulation was performed through a radiant heat apparatus (Ugo Basile, #7360, Gemonio, Varese, Italy; I.R. intensity $= 30$ mW/cm^2). The cutoff latency was set for 20 s to avoid heating-induced tissue damage when the thermal stimulation was gradually increased. As soon as the rat lifted his paw heated, the stimulation stopped immediately, and the TWL was determined accordingly. Two or three experimenters performed the behavioral tests, and only one of them was not "blind" to the experimental design and condition of the rat under investigation. Each of them provided his/her evaluation. The same assessments provided at least by two experimenters were used for the data analysis.

BMSC cultures and flow cytometric analysis

BMSCs obtained from donor rats under aseptic conditions were cultured (see Supplementary Figure 1), as described previously.[20] In brief, after rats were sacrificed with 4% chloral hydrate, both ends of the tibiae, femurs, and humeri were cut off by scissors. Bone marrow was flushed out with a culture medium consisting of

Dulbecco's modified Eagle's medium (Gibco, Grand Island, NY, USA) and 10% fetal bovine serum (Gibco) through a syringe fitted with an 18-gauge needle and inserted into the shaft of the bone. After the mechanical dissociation of the bone marrow, debris was removed with a 100-μm cell filter. Cells were then incubated at 37°C in 5% CO_2 in tissue-culture flasks (25 mm^2) (Corning, NY, USA). The culture medium was changed in 48 hr to remove nonadherent cells. The culture medium was changed every other day thereafter. On day 7, when the cultures reached 80% confluence (see Supplementary Figure 1(a)), the cells were washed with phosphate-buffered saline (PBS) and harvested by incubation with 1 ml of 0.25% trypsin/1 mM ethylenediaminetetraacetic acid at 37°C for 7 min. The culture medium was added to neutralize trypsin. Cells were then centrifuged at 1,000 g for 7 min and washed with PBS.

For assessing the properties of collected cells, the cells were incubated in a solution saturated with fluorescein isothiocyanate (FITC)-conjugated monoclonal antibodies against CD45 (1:200, AB_2572455, eBioscience, Shanghai, China) and CD90 (1:200, AB_465151, eBioscience) for 20 min on ice in the dark. Incubation in a solution saturated with isotype-matched FITC-conjugated mouse IgG1 kappa (1:200, AB_10596964, eBioscience) or IgG2a kappa (1:200, AB_470027, eBioscience) was performed as isotype control. After washing for three times with 0.01 M PBS, cells were centrifuged at 400 g for 5 min and resuspended in a 0.5 ml ice-cold 0.01 M PBS. The fluorescence staining of cells was evaluated by using an FC500 flow cytometer (Beckman Coulter, Brea, CA, USA). The data were analyzed using FlowJo 8.8.6 (TreeStar Inc., Ashland, OR, USA) (see Supplementary Figure 1(b)). BMSCs (1×10^6 cell in 0.3 ml PBS) were delivered intravenously into rats through one tail vein over a 2-min period using a 22-gauge needle.

Lentivirus particle delivering

Lentivirus particles (1×10^8 plaque forming units (PFU)/ml, 10 μl) conjugated with IL-33 siRNA 5'-ATGATGAGAGCTGTAACAATA-3' (sh-IL-33, Genechem, Shanghai, China, www.genechem.com.cn, see Table 1)[21] or the nonspecific negative control sequence 5'-TTCTCCGAACGTGTCACGT-3' (sh-NC, Genechem, see Table 1)[21–23] was intrathecally injected as previously described.[7] In brief, after rats were anesthetized with 3% isoflurane (YaJi Biological, Shanghai, China), a 26-gauge needle connected to a 10-μl microinjection syringe was inserted into the intervertebral space between the lumbar 4 (L4) and L6 regions. The tail-flick reflex was considered to be an indicator of the accuracy of each intrathecal (i.t.) injection. The dorsal root ganglion (DRG) and SDH tissues of L4 to L6 were sampled on days 3 and 7 after the i.t. injection to examine the effect of sh-IL-33 delivered.

Vector construction and dual-luciferase reporter assay

About 200-bp sequences of IL-33–3' untranslated region (UTR) and ST2-3' UTR containing the predicted miR-547-5p binding sites and their mutant sequences (see Table 1) synthesized by Genewiz Company (Suzhou, China, www.genewiz.com.cn) were cloned into KpnI and XhoI sites of the pGL3-control expression vector (Promega, Madison, WI, USA), respectively. The resulting constructs were verified by direct sequencing. For the dual-luciferase reporter assay, HEK293T cell line (Hanbio Biotechnology, Shanghai, China) was dispensed into 24-well plates at a density of 50,000 cells per well the day before transfection. The constructed wild-type or mutant-type vector (500 ng) and the miR-547-5p mimic (100 nM, RiboBio, Guangzhou, China; www.ribobio.com) (see Table 1) as well as pRL-TK vector (50 ng, Promega) were cotransfected using Lipofectamine 6000 (Beyotime Biotechnology, Shanghai, China) according to the manufacturer's protocol. miRNA mimic negative control (100 nM, RiboBio) (see Table 1) was used as a negative control in every transfection experiment. After 24 hr, the firefly luciferase activity normalized with the renilla luciferase in cell lysate was measured with the Dual-Luciferase Assay System in TD-20/20 Luminometer (Turner BioSystems, CA, USA). Five replicates were done for each group, and the experiment was repeated at least three times. Changes in the normalized luciferase activity relative to that in cells cotransfected with plasmids encoding the mimic control and *IL-33* wild type or *ST2* wild type (= 1, dashed line in Figure 1(d) and (e)) were calculated.

Real-time polymerase chain reaction analysis

Total RNAs were extracted from DRG or SDH tissues using the TRIzol reagent (Thermo, Shanghai, China) according to the manufacturer's instructions. The RNA was reversed and transcribed into cDNA using the random hexamer primers (Bimake.cn, Shanghai, China). A template (2 μl) was used for amplification by real-time polymerase chain reaction (PCR) with the random hexamers, oligo (dT) primers, or specific RT primers, as shown in Table 1. The expression of glyceraldehyde-3-phosphate dehydrogenase (GAPDH, Genewiz) or U6 (RiboBio) was used as internal controls for normalization. Each sample was run in a 20-μl volume for reaction with forward and reverse primers (250 nM) (see Table 1), 2× SYBR Green qPCR Master Mix (10 μl, Bimake.cn), and total cDNAs (20 ng). For miRNA quantitative real-time reverse transcription

Table 1. Sequences used in the current study.

| Agent	Sequences	Manufactures
Primer of IL-33	Forward: 5′-CCCTGAGCACATACAACGACC-3′ Reverse: 5′-CACCATCAGCTTCTTCCCATC-3′	Genewiz, Suzhou, China; www.genewiz.com.cn[21]
1363–1575 of IL-33 DNA (WT)	CATCGCTATATGCCCCAGGCACCCCTCAGATCA GCCCTTTCTGTCAAGAACCCTAGCACTCCAGATGTC TACATGTCTAGACAGACAAGTCTGTGTTTG**TGAAGTG** GATGATATTACCTCTTGTTTCCTTCTTAAAATTCCATTT TTTTTTCAACACAGCAACTTAACTTTAAGCAAGCCAGC TTACATTAGGAAACGAAACACATTT	Genewiz, Suzhou, China; www.genewiz.com.cn
1363–1575 of IL-33 DNA (MT)	CATCGCTATATGCCCCAGGCACCCCTCAGATCAGCCC TTTCTGTCAAGAACCCTAGCACTCCAGATGTCTACAT GTCTAGACAGACAAGTCTGTGTTTG**ACTTCAC**GAT GATATTACCTCTTGTTTCCTTCTTAAAATTCCATTTTTT TTTCAACACAGCAACTTAACTTTAAGCAAGCCAGCTT ACATTAGGAAACGAAACACATTT	Genewiz, Suzhou, China; www.genewiz.com.cn
Primer of ST2	Forward: 5′-TCAGTTCGTTGCTGTCCTGT-3′ Reverse: 5′-TGGAACTTTTATTTGGGCCTTTCT-3′	Genewiz, Suzhou, China; www.genewiz.com.cn
1981–2065 of ST2 DNA (WT)	GGTTGCTTGGACCTGAAACACTTTTGAGTCGTGGACTT GCCTACTCAGAGCTGGGGAATCCCAGCAGTAGGCC CCA**GAAGTG**AAGGTGTGAAGACTTGAAATGC CAAGGGTGGGGCCCC	Genewiz, Suzhou, China; www.genewiz.com.cn
1981–2065 of ST2 DNA (MT)	GGTTGCTTGGACCTGAAACACTTTTGAGTCGTGGACTT GCCTACTCAGAGCTGGGGAATCCCAGCAGTAGGCC CCA**CTTCAC**AAGGTGTGAAGACTTGAAATGCCAAGGG TGGGGCCC	Genewiz, Suzhou, China; www.genewiz.com.cn
rno-miR547-5p Mimic	5′-UCACUUCAGGAUGUACCACCCA-3′ 3′-AGUGAAGUCCUACAUGGUGGGU-5′	RiboBio Co., Ltd., Guangzhou, China; www.ribobio.com
Mimic control	5′-UUUGUACUACACAAAAGUACUG-3′ 3′-AAACAUGAUGUGUUUUCAUGAC-5′	RiboBio Co., Ltd., Guangzhou, China; www.ribobio.com[24]
Sh-IL-33	5′-ATGATGAGAGCTGTAACAATA-3′	Gene Chemical Co., Ltd., Shanghai, China; www.genechem.com.cn[21]
Sh-NC	5′-TTCTCCGAACGTGTCACGT-3′	Gene Chemical Co., Ltd., Shanghai, China; www.genechem.com.cn[21–23]
Agomir-547-5p	5′-UCACUUCAGGAUGUACCACCCA-3′ 3′-GGUGGUACAUCCUGAAGUGAUU-5′	GenePharma, Shanghai, China; www.genepharma.com
Agomir-NC	5′-UUCUCCGAACGUGUCACGUTT-3′ 3′-ACGUGACACGUUCGGAGAATT-5′	GenePharma, Shanghai, China; www.genepharma.com[25–27]
Antagomir-547-5p	5′-UGGGUGGUACAUCCUGAAGUGA-3′	GenePharma, Shanghai, China; www.genepharma.com
Antagomir-NC	5′-CAGUACUUUUGUGUAGUACAA-3′	GenePharma, Shanghai, China; www.genepharma.com[28]
Primer of GAPDH	Forward: 5′-AGGTCGGTGTGAACGGATTTG-3′ Reverse: 5′-GGGGTCGTTGATGGCAACA-3′	Genewiz, Suzhou, China; www.genewiz.com.cn[29]

IL-33: interleukin-33; ST2 suppressor of tumorigenicity 2; WT: wild type; MT: mutant type in which the interaction sites with miR547-5p were mutated; NC: nonspecific negative control sequence; rno-miR547-5p: rat noncoding miRNA-547-5p; Sh-IL-33: lentivirus particles conjugated with short hairpin RNA which inhibits the expression of IL-33 protein. Bolded and underlined nucleotides in the wild type of IL-33 or ST2 indicate (also see Figure 1(a)) the interaction sites with miR547-5p predicted with TargetScan (http://www.targetscan.org/).

PCR, an miRcute miRNA qPCR Detection Kit (TIANGEN, Beijing, China) was used. Reactions were implemented in a 7500 Fast Real-Time PCR Detection System (Applied Biosystems, Foster City, CA, USA). All IL-33 and ST2 data were normalized to GAPDH, and all miR-547-5p data were normalized to U6, which was confirmed to be stable. The ratios of the mRNA levels in rats were calculated using the $2^{[-\text{DeltaDeltaC(T)}]}$ method.[30,31]

Western blot analysis

Western blotting experiments were performed as described previously.[18,19,32] In brief, tissues isolated
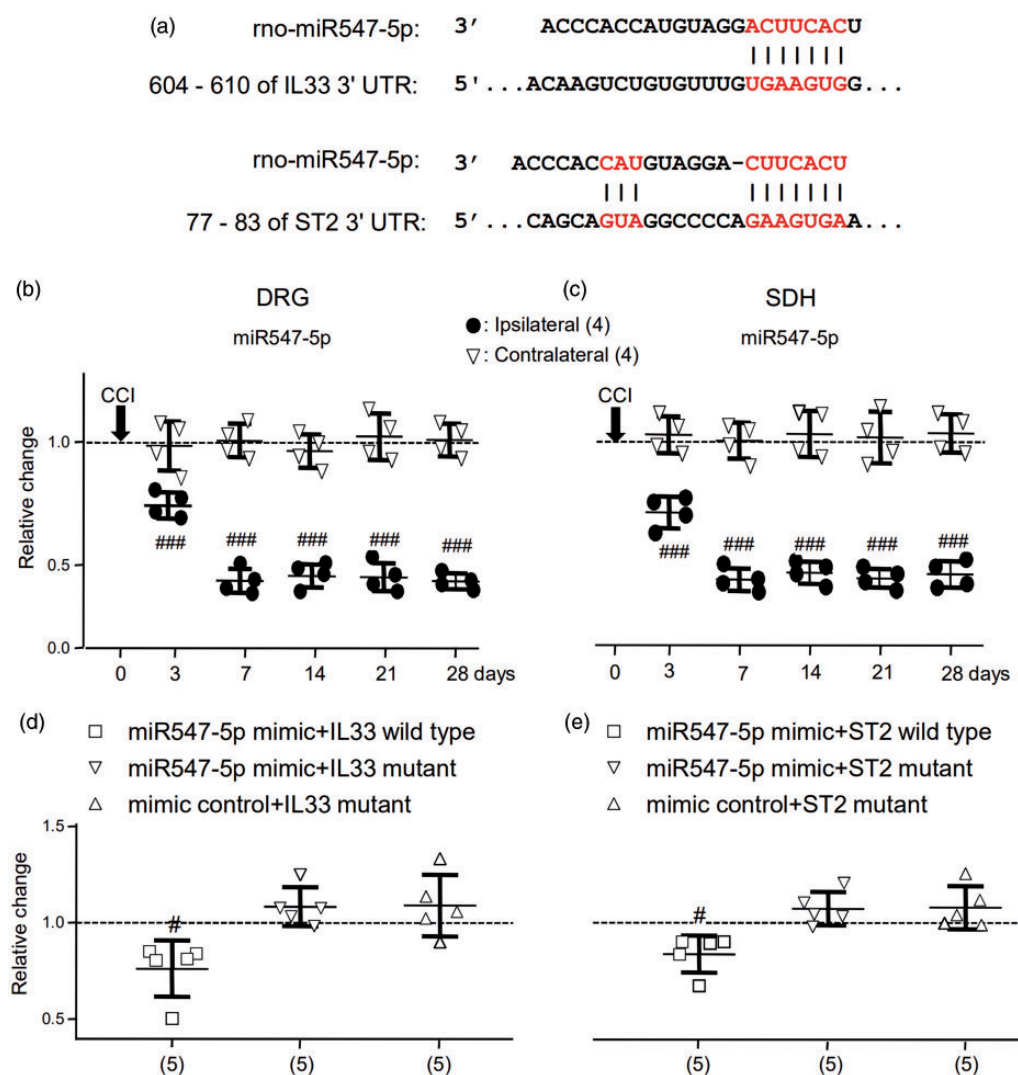
Figure 1. The expression of miR-547-5p (miR547-5p) was increased following the CCI and directly interacted with IL-33–3' UTR and ST2-3' UTR. (a) The regions (red) of the matched seed predicted with the TargetScan software. (b) and (c) Summary data (mean ± SD) showing the relative changes in the expression of miR547-5p in the DRG (b) and SDH (c) after the CCI to that in naive rats (dashed line, = 1). DRG: The L4 to L6 DRG of the spinal cord. SDH: The L4 to L6 dorsal horn of the spinal cord. Ipsilateral: The DRG or SDH ipsilateral to the CCI. Contralateral: The DRG or SDH contralateral to the CCI. ###$p < 0.001$ (Bonferroni's post hoc test in two-way ANOVA of the ipsilateral versus contralateral DRG or SDH. (d) and (e) Summary data (mean ± SD) showing relative changes in the luciferase activity in HEK293T cells cotransfected with plasmids encoding the mimic control and *IL-33* wild type or *ST2* wild type (dashed line, = 1; see Table 1). #$p < 0.05$, Bonferroni's post hoc test in one-way ANOVA of data versus that in cells cotransfected with plasmids of the mimic control and *IL-33* wild type or *ST2* wild type (Table 1). Values in brackets indicate the number of rats tested.
miRNA: microRNA; IL33: interleukin-33; UTR: untranslated region; ST2: suppressor of tumorigenicity 2; DRG: dorsal root ganglia; SDH: spinal dorsal horn.

from the DRG or SDH were homogenized in an ice-cold radioimmunoprecipitation assay buffer (Beyotime Biotechnology) supplemented with protease inhibitor cocktail (Bimake.cn), phosphatase inhibitor cocktail (Bimake.cn), phenylmethylsulfonyl fluoride (PMSF, Beyotime Biotechnology), and dithiothreitol (DTT, 0.5 mM, Beyotime Biotechnology). After the homogenates were centrifuged at 12000 g for 20 min at 4°C, protein concentrations were determined with bicinchoninic acid (BCA) assay (Beyotime Biotechnology). Loading buffer (5×, Thermo) were added to generate samples subjected to sodium dodecyl sulphate-polyacrylamide gel electrophoresis. Sampled proteins (50 μg) were loaded into each lane of the gel. Proteins transferred to 0.45 μm polyvinylidene fluoride membranes (Millipore, Suzhou, China) were then repeatedly stripped and successively probed with antibodies for overnight at 4°C). Rabbit IL-33 antibody (1:1000, AB_2827630, Abcam,

Cambridge, MA, USA), rabbit ST2 antibody (1:1000, AB_2827695, Novus, Centennial, CO, USA), and tublin antibody (1:2000, AB_2210695, Proteintech, Wuhan, China) were used. The primary antibody staining was visualized with the probe of peroxidase-conjugated goat anti-rabbit IgG (1:1000, AB_2313567, Thermo, Waltham, MA, USA) for 2 hr at room temperature. Stripping effects were carefully examined before successive antibody probing. The stripping was thought to be successful if no specific staining signal could be detected through incubation with a secondary antibody but without the incubation of a primary antibody. Densitometry analyses of Western blot bands were done with Bio-Rad image software (Bio-Rad, Shanghai, China). Samples from naive animals that did not receive any treatment were examined in biochemical experiments for controlling variations that may occur in biochemical experiments. The probe with the tublin antibody (Proteintech) was conducted as a loading control. The ratio of the band intensity versus that of tublin was calculated and then normalized to the ratio in naive rats or rats that received treatment with nonspecific negative control (NC, see Table 1) for examining relative changes induced by any treatment.

Immunofluorescence image

On day 7, after the CCI operation, the rats were sacrificed with 4% chloral hydrate and then perfused intracardially with 0.01 M PBS followed by 4% paraformaldehyde in 0.1 M PBS (pH 7.4). The DRG or spinal cord from L4 to L6 was sampled and fixed for 12 hr with 4% paraformaldehyde and then dehydrated by the gradient of 15% and then 30% sucrose. The DRG or spinal cord was frozen and sectioned on a freezing-microtome (Leica 2000, Wetzlar, Germany) at a thickness of 15 μm for immunofluorescence staining. The specificities of the antibodies used were examined by the Western blotting analysis or omission of the primary antibodies. After washing for three times and blocking with 4% donkey serum (MultiSciences, Hangzhou, China) in 0.3% Triton X-100 (Beyotime Biotechnology) for 1 hr at 37°C, the sections were incubated overnight at 4°C with a primary antibody in PBS added with 1% normal donkey serum and 0.3% Triton X-100. Rabbit IL-33 antibody (1:500, AB_2827630, Abcam), rabbit ST2 antibody (1:100, AB_2540840, Thermo), mouse glutamine synthetase (GS) antibody (1:200, AB_1140869, Abcam), mouse NeuN antibody (1:200, AB_2298772, Merck Millipore, Billerica, MA), and mouse GFAP antibody (1:300, AB_561049, Cell Signaling Technology, Danvers, MA) were used for primary staining. For visualization of the primary staining, the sections were washed with PBS and incubated with Cy3-conjugated goat anti-rabbit IgG (1: 300,

AB_2716305, Boster, Wuhan, China) or Dylight 488 goat anti-mouse IgG (1:300, AB_2827694, Boster) for 1 hr at 37°C. Fluorescence images were captured under an inverted fluorescence microscope (Eclipse Ni-U, Nikon, Tokyo, Japan) equipped with a CCD camera (DS-Fi1c, Nikon) by using the software NIS-Elements F4.6 (Nikon). The image data were analyzed with the software Image-Pro Plus (Version 6.0, Media Cybernetic, Rockville, MD, USA). All chemicals used in this study were purchased from Sigma (Shanghai, China) except for those as indicated. All data, materials, and protocols are fully available to readers without undue qualifications in transfer agreements.

Statistical analysis

All data are expressed as mean ± standard deviation (SD). Unpaired t test, Mann–Whitney U test, or one- or two-way analysis of variance (ANOVA) were carried out for the data analysis; $p < 0.05$ was considered statistically significant.

Results

CCI significantly reduced the expression of the miR-547-5p, which directly interacted with both the IL-33 and ST2 mRNAs in HEK293T cells, in the DRG and SDH

Since the vast majority of identified miRNAs regulate the function of mRNAs through the interaction with canonical sites, to clarify mechanisms that may underlie the upregulation of IL-33/ST2 signaling associated with tissue injury such as CCI, we used TargetScan (http://www.targetscan.org/).[33] Based on the overlapped data from TargetScan, it was found that the seed sequence of the miR-547-5p position (2–8) was paired with IL-33 and ST2 3' UTR from 606 to 610 and 77 to 83 bps, respectively (see Figure 1(a)). Importantly, we found that the expressions of miR-547-5p in the ipsilateral L4 to L6 of both the DRG and SDH of rats were significantly ($p < 0.001$, $F(5, 18) = 113.5$ and 98.5) reduced following the CCI (Figure 1(b) and (c)). In contrast, the expressions of miR-547-5p in the contralateral DRG and SDH were not significantly ($p = 0.856$ and $p = 0.99$, $F(5, 18) = 0.38$ and 0.11) changed after the CCI (Figure 1(b) and (c)). When compared with those in the contralateral DRG and SDH, the expressions of miR-547-5p in the ipsilateral DRG and SDH were significantly ($p < 0.001$, $F(5, 30) = 50.06$ and 24.52) reduced at day 3 after the CCI, and the reduction lasted till day 28 (see Figure 1 (b) and (c)).

Furthermore, it was confirmed that miRNA547-5p might regulate *IL-33* or *ST2* through direct binding to their 3' UTRs in a dual-luciferase reporter assay. The

wild or mutant 3′ UTR of *IL-33* or *ST2* (see Table 1) was inserted into the downstream region of the pGL3-control luciferase reporter gene. Plasmids of the miR-547-5p mimic and pGL3-control constructs (see Table 1) were cotransfected into HEK293T cells. The luciferase activity relative to that in HEK 293 T cells cotransfected with plasmids encoding the mimic control and *IL-33* wild type or *ST2* wild type (= 1, dashed line in Figure 1(d) and (e)) was calculated. We found that the relative luciferase activity was significantly reduced in cells cotransfected with the miR-547-5p mimic and *IL-33* wild type or *ST2* wild type by $24 \pm 15\%$ or $15 \pm 10\%$ (mean $\pm$ SD; $p < 0.05$, $F(3, 19) = 8.23$ or 9.85; Figure 1 (d) and (e)). No significant change in the relative luciferase activity could be found in cells cotransfected with the miR-547-5p mimic and mutant *IL-33* or *ST2,* or the mimic control and mutant *IL-33* or *ST2* (Figure 1(d) and (e)). The significant decreases detected in the luciferase activity suggested that miR-547-5p might specifically bind to either *IL-33* or *ST2* and regulate both the *IL-33* and *ST2* in HEK293T cells.

Via depressing miRNA-547-5p (miR-547-5p), CCI induced the upregulation of IL-33/ST2 signaling in both the DRG and SDH, and pain hypersensitivity

We then examined the distributions of IL-33 and ST2 in the DRG (see Supplementary Figure 2) and SDH (see Supplementary Figure 3) of rats with the CCI. The colocalization of IL-33 and GS or GFAP antibody staining could be found in both the DRG and SDH, but no colocalization of IL-33 and NeuN antibody staining could be found (see Supplementary Figures 2 and 3). The ST2 antibody staining was found to be colocalized with NeuN in both the DRG and SDH (see Supplementary Figures 2 and 3) but not with GS antibody staining in the DRG (see Supplementary Figure 2).

When compared with that in the DRG contralateral to the CCI, the expressions of IL-33 and ST2 mRNAs in the ipsilateral DRG were significantly increased at day 3 after the CCI ($p < 0.05$, $F(5, 40) = 10.02$ and 6.14). The increases lasted till day 28 (see Figure 2(a) and (b)). The increases in the expression of IL-33 and ST2 proteins were found in the DRG at day 7 (see Figure 2(c) to (f)) and lasted till days 28 and 14, respectively (see Figure 2(c) to (f)).

When compared with that in the SDH contralateral to the CCI, significant increases in the expressions of IL-33 and ST2 mRNAs were found at days 7 and 3 (see Figure 3(a) and (b); $p < 0.001$, $F(5, 40) = 10.76$ and 9.08), respectively. Increases in the expression of IL-33 and ST2 proteins were found at day 7 ($p < 0.001$, $F(5, 30) = 6.34$ and 6.31; see Figure 3(c) to (f)).

We then examined effects of altering the expression of endogenous miR-547-5p by i.t. infusion of the miR-547-5p agomir (Agomir-547-5p, Table 1; 20 μM), antagomir (Antagomir-547-5p, Table 1; 20 μM), or their control (Agomir-NC or Antagomir-NC; see Table 1) once daily for consecutive four days (see Supplementary Figure 4(a)) into the region between the L4 and L6 of the spinal cord. When compared with the expression of miR-547-5p in naive rats, no significant change was found in the right L4 to L6 DRG (see the left graphs in Figure 4(a) and (b)) and SDH (see the left graphs in Figure 4(c) and (d)) of rats that received only agomir-NC (Table 1, 20 μM; Figure 4(a) and (c)) or antagomir-NC (Table 1, 20 μM; Figure 4(b) and (d)). However, when compared with the effects of agomir-NC, the i.t. administration of agomir-547-5p increased the expression of endogenous miR-547-5p in the DRG by $176 \pm 16\%$ (mean $\pm$ SD, $n = 4$ rats; Figure 4(a); $p < 0.001$, $t(6) = 21.5$), whereas the antagomir-547-5p administration reduced the expression of miR-547-5p by $59 \pm 11\%$ (mean $\pm$ SD, $n = 4$ rats; Figure 4(b), $p < 0.001$, $t(6) = 10.4$) when compared with the effect of the i.t. administration of the antagomir-NC. Similarly, the expression of miR-547-5p in the SDH was increased by $139 \pm 18\%$ following the infusion of agomir-547-5p (mean $\pm$ SD, $n = 4$ rats; Figure 4(c); $p < 0.001$, $t(6) = 15.9$) but reduced by $53 \pm 13\%$ following the infusion of antagomir-547-5p (mean $\pm$ SD, $n = 4$ rats; Figure 4 (d), $p < 0.001$, $t(6) = 7.8$).

The i.t. infusion of agomir-547-5p into naive rats (see Supplementary Figure 4(a)) did not produce any significant effect on the expression of mRNAs or proteins of IL-33 and ST2 (see Figure 4(e) to (n)). However, the increases in the expressions of IL-33 and ST2 mRNAs or proteins in the ipsilateral DRG (see Figure 4(e), (f), (i), (k), (l)) and SDH (see Figure 4(g), (h), (j), (m), (n)) induced by the CCI were significantly reduced by the agomir-547-5p infusion when compared to those in the animals that received the agomir-NC administration (see Supplementary Figure 4 (b)). Furthermore, our data showed that the administration of agomir-547-5p significantly diminished the reduction of the MWT and TWL induced by the CCI (see Figure 4(o), $p < 0.001$, $F(5, 70) = 25.2$ and 50.7). In contrast, no effect on the MWT and TWL could be found after the administration of agomir-547-5p in naive animals (see Supplementary Figure 4(c)).

We then examined the effects of the i.t. administration of antagomir-547-5p. When compared with those in naive animals, the i.t. administration of antagomir-NC (see Supplementary Figure 4(a)) produced no change in the expression of miR-547-5p, IL-33, and ST2 mRNAs (see the left graphs in Figure 5(a) to (d)) and proteins (see Figure 4(i) and (j); the left graphs in Figure 5(g) to (j)). In contrast, the i.t. administration of antagomir-547-5p not only reduced the expression of miR547-5p (see the right graphs of Figure 4(b) and (d)) but also caused increases in the expression of IL-33 and ST2 mRNAs
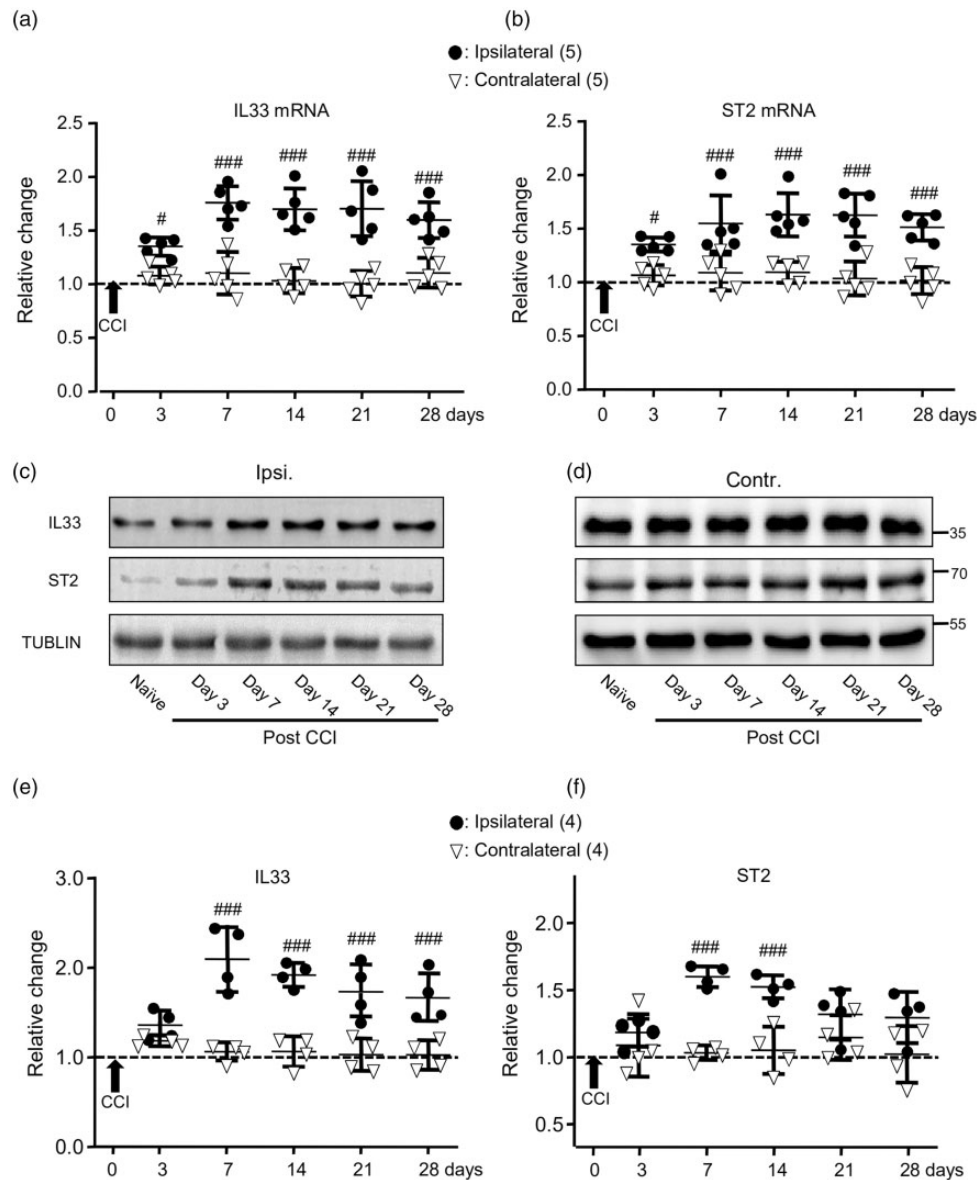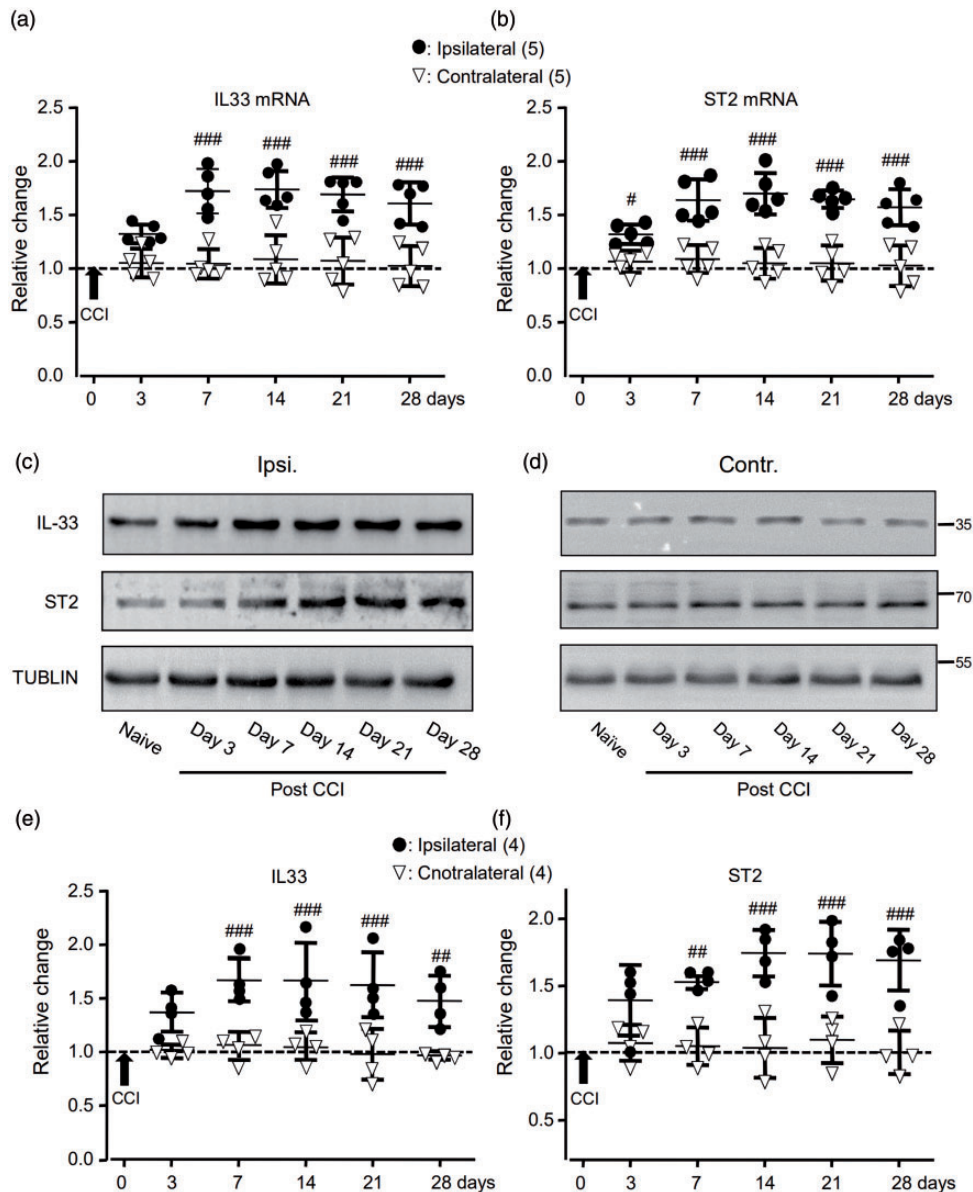
Figure 2. The expressions of IL-33 (IL33) and ST2 mRNAs and proteins in the DRG were increased following the CCI. (a) and (b) Summary data (mean ± *SD*) showing the relative changes in the expression of IL-33 (a) and ST2 (b) mRNAs after the CCI to that in naive rats (dashed line, = 1). #$p < 0.05$, ###$p < 0.001$, Bonferroni's post hoc test in two-way ANOVA of ipsilateral versus contralateral DRG. (c) and (d) Examples of Western blot. Gels (from left to right) in (c) and (d) were respectively loaded with lysates prepared from the right L4 to L6 DRG of naive rats without any treatment (naive) or ipsilateral (ipsi.) or contralateral (contr.) DRG of rats on days 3, 7, 14, 21, and 28 after the CCI. Each group of the blots was stripped and successively probed with antibodies as indicated on the left of blots in (c). Values on the right side of blots in (d) indicate the molecular mass (Kd). (e) and (f) Summary data (mean ± *SD*) showing the relative changes in the expression of IL-33 (e) and ST2 (f) proteins in the DRG. The ratio of band intensities versus that of tublin was calculated and then normalized to the ratio in naive animals (= 1, dashed line) for determining relative changes. ###$p < 0.001$, Bonferroni's post hoc test in two-way ANOVA of ipsilateral versus contralateral DRG of rats after the CCI.
IL33: interleukin-33; miRNA: microRNA; ST2: suppressor of tumorigenicity 2; CCI: constriction nerve injury.

(see the right graphs in 5(a) to (d)) and proteins (see Figure 5(e) and (f); the right graphs in Figure 5(g) to (j)) in both the DRG and SDH of animals when compared to those in animals that received the administration of antagomir-NC (see Figure 5(a) to (j)).

In consistency, the i.t. administration of the antagomir-NC did not produce any change in the MWT and TWL ($p = 0.84$ and $p = 0.8$, $F(4, 20) = 0.36$ and 0.4, Figure 5(k)). When compared to that induced by the i.t. administration of antagomir-NC, the MWT

Figure 3. The expressions of IL-33 (IL33) and ST2 mRNAs and proteins in the SDH were increased following the CCI. (a) and (b) Summary data (mean $\pm$ SD) showing the relative changes in the expression of IL-33 (a) and ST2 (b) mRNAs after the CCI to that in naive rats (dashed line, = 1). #$p < 0.05$, ###$p < 0.001$, Bonferroni's post hoc test in two-way ANOVA of ipsilateral versus contralateral SDH. (c) and (d) Examples of Western blots. Gels (from left to right) in (c) and (d) were respectively loaded with lysates prepared from the right L4 to L6 SDH of naive rats without any treatment (naive) or ipsilateral (ipsi.) and contralateral (contr.) SDH of rats on days 3, 7, 14, 21, and 28 after the CCI. Each group of the blots was stripped and successively probed with antibodies as indicated on the left of blots in (c). Values on the right side of blots in (d) indicate the molecular mass (Kd). (e) and (f) Summary data (mean $\pm$ SD) showing the relative changes in the expression of IL-33 (e) and ST2 (f) proteins in the SDH. The ratio of band intensities versus that of tublin was calculated and then normalized to the ratio in naive animals (= 1, dashed line) for determining relative changes. ##$p < 0.01$, ###$p < 0.001$; Bonferroni's post hoc test in two-way ANOVA of ipsilateral versus contralateral SDH of rats after the CCI.
IL33: interleukin-33; ST2: suppressor of tumorigenicity 2; miRNA: microRNA; CCI: constriction nerve injury.

and TWL were significantly reduced after the i.t. administration of antagomir-547-5p (see Figure 5(k), $p < 0.001$, $F(4, 40) = 86.21$ and 102.6).

These findings strongly implied that the depression of miR-547-5p might act as an upstream signal for inducing

the enhancement of IL-33/ST2 signaling and thereby causing pain hypersensitivity in the CCI model. To exam this hypothesis, we then investigated the effects of the upregulation of IL-33 on the expression of miR-547-5p. Although the one-time i.t. infusion of
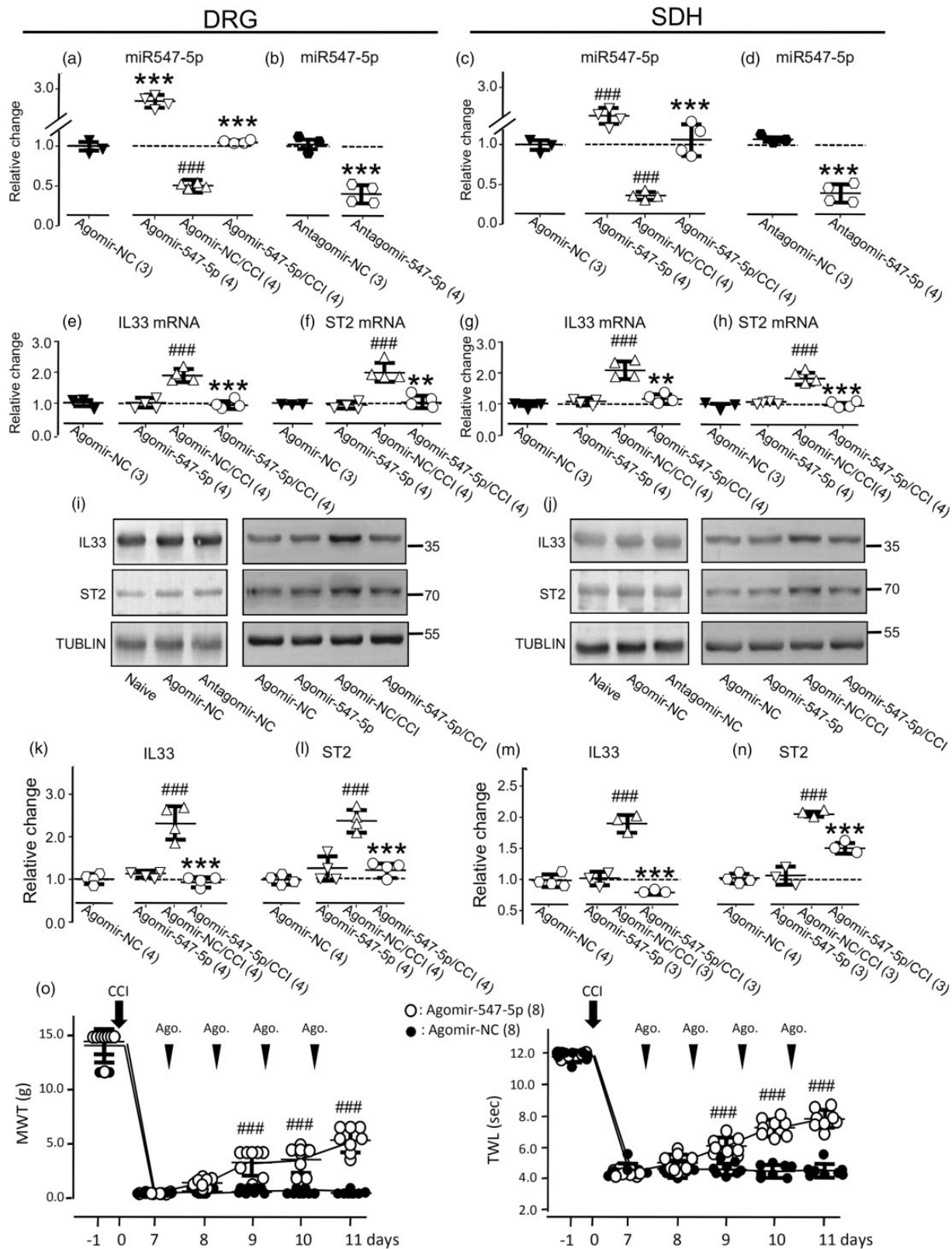
Figure 4. Effects of altering the expression of miR-547-5p (miR547-5p) by the intrathecal (i.t.) administration of agomir-miR-547-5p (agomir-547-5p) or antagomir-miR-547-5p (antagomir-547-5p). The left graphs of (a) and (c): Summary data (mean $\pm$ *SD*) showing the expression of miR547-5p in rats that received agomir-NC (20 μM, see Supplementary Figure 4(a)), which were normalized to that in naive rats without any treatment ($= 1$, dashed line). The right graphs of (a) and (c): Summary data (mean $\pm$ *SD*) showing the expression of

recombinant IL-33 (rIL-33; Novus Biologicals, Littleton, CO, USA; http://www.novusbio.com)[7,34] at dose 10, 30 or 100 ng produced a dose-dependent reduction of the MWT from 14.3 ± 1.0 g to 11.8 ± 0.9, 9.3 ± 1.3 or 6.1 ± 0.9 g (mean $\pm$ SD, $n = 6$ rats; $p < 0.001$, $F(2, 15) = 44.58$) and the TWL from 11.9 ± 0.1 s to 7.9 ± 0.3, 6.4 ± 0.3 or 5.0 ± 0.2 s (mean $\pm$ SD, $n = 6$ rats; $p < 0.001$, $F(2, 15) = 166.9$) 3 hr after the infusion, the item (100 ng once daily for 4 consecutive days, see Supplementary Figure 5(a)) produced no significant change in the expression of miR-547-5p in the right L4 to L6 DRG (Figure 6(a); $p = 0.59$, $t(6) = 0.57$) or SDH (Figure 6(a); $p = 0.61$, $t(6) = 0.54$) when compared to those of naive rats. Thus, it was implied that the expression of miR-547-5p was unlikely a downstream event regulated by IL-33 at the dose which could significantly alter somatosensitivity.

We then examined the effects of the downregulation of IL-33. For this aim, lentivirus particles (1×10^{8} PFU/ml) conjugated with GFP and IL-33 siRNA 5'-ATGATGAGAGCTGTAACAATA-3' (sh-IL-33, Gene Chemical Co., Ltd., Shanghai, China; www.genechem.com.cn; see Table 1)[21] or a nonspecific negative control sequence 5'-TTCTCCGAACGTGTCACGT-3' (sh-NC, see Table 1)[21–23] were i.t. infused in the region between the L4 to L6 of the spinal cord of rats. Supplementary Figure 6 shows the colabeling of endogenous IL-33 detected with IL-33 antibody (red) and lentivirus particles conjugated with GFP and sh-IL-33 (green) infused intrathecally.

The Western blot analysis showed that compared to those in naive rats, no change in the expression of IL-33 protein in both the DRG and SDH was found after the infusion of sh-NC (see Figure 6(b) to (e)). When compared with that of animals that received the infusion of the sh-NC, IL-33 protein expressions in both the DRG and SDH were significantly reduced at days 3 and 7 following the i.t. infusion of sh-IL-33 (see Figure 6(b) to (e)).

The infusion of sh-IL-33 into naive rats did not induce any significant change in the expressions of ST2 (see Figure 6(b) to (e)) and miR-547-5p (see Figure 6(f) and (g)). Interestingly, however, the CCI (see Supplementary Figure 5(b)) still induced significant depression of miR-547-5p in both the DRG and SDH (see Figure 6(f) and (g); $p < 0.001$, $t(6) = 8.2$ and 8.5) of animals in which the expression of IL-33 had been knocked down. Taken together, we concluded that the upregulation of IL-33/ST2 signaling, which caused pain hypersensitivity, was a downstream event induced by the depression of miR-547-5p.

BMSC application significantly reduced pain hypersensitivity via blocking the depression of miR-547-5p and the upregulation of IL-33/ST2 signaling

Recent studies have shown that BMSCs may produce long-lasting analgesic effects in animal models of chronic pain, such as neuropathic pain.[15–17] However, the underlying mechanisms remain largely unknown. In this

Figure 4. Continued

miR547-5p, which were normalized to that in rats that received agomir-NC (20 μM, = 1, dashed line, see Supplementary Figure 4(a)). The left graphs of (b) and (d): Summary data (mean $\pm$ SD) showing the expression of miR547-5p in rats that received antagomir-NC (20 μM, see Supplementary Figure 4(a)) which were normalized to that in naive rats (= 1, dashed line). The left graphs in (e), (f), (g), and (h): Summary data (mean $\pm$ SD) showing IL-33 and ST2 mRNAs in the DRG (e, f) and SDH (g, h), which were normalized to that in naive rats. The right graphs in (e), (f), (g), and (h) show the expression of IL-33 and ST2 mRNAs, which were normalized to that of rats that received the i.t. administration of agomir-NC. (i) and (j) Examples of Western blots. Gels (from left to right) in (i) and (j) were respectively loaded with lysates prepared from the right L4 to L6 DRG (i) and SDH (j) of naive rats without any treatment (naive), or the right (ipsilateral) L4 to L6 DRG (i) and SDH (j) of rats with or without the CCI received the i.t. administration of agomir-NC, antagomir-NC, or agomir547-5p as indicated. Each group of the blots was stripped and successively probed with antibodies as indicated on the left of blots. Values on the right side of blots indicate the molecular mass (Kd). (k) to (n) Summary data (mean $\pm$ SD) showing the relative changes in the expression of IL-33 (k, m) and ST2 (l, n) proteins in the DRG (k, l) and SDH (m, n). The ratio of band intensities versus that of tublin was calculated and then normalized to the ratio in naive animals (= 1, dashed line) was shown in the left graphs of (k) to (n). The ratio normalized to that in rats that received the i.t. agomir-NC administration (= 1, dashed line) was shown in the right graphs of (k) to (n). Agomir-NC/CCI: agomir-NC (20 μM) was i.t. infused into rats after the CCI (see Supplementary Figure 4(b)); Agomir-547-5p/CCI: agomir-547-5p (20 μM) was i.t. infused into rats after the CCI (see Supplementary Figure 4(b)). (o) Summary data (mean $\pm$ SD) showing the effects of the i.t. administration of agomir-NC (20 μM) or agomir-547-5p (20 μM) once daily for four consecutive days on the MWT, and TWL of rats that received the CCI. A black arrow indicates the CCI. The black arrowheads indicate the i.t. infusion of agomir-NC or agomir-547-5p. ###$p < 0.001$, Bonferroni's post hoc test in one-way ANOVA in comparison with that of the i.t. agomir-NC administration. **$p < 0.01$, ***$p < 0.001$, unpaired t test in comparison of the effects of the i.t. agomir-547-5p versus agomir-NC administration in rats without or with CCI in (a), (c), (e) to (h), (k) to (n), or the effects of the i.t. antagomir-547-5p versus antagomir-NC administration in (b) and (d). Values in brakes indicate the number of rats tested.

DRG: dorsal root ganglia; SDH: spinal dorsal horn; CCI: constriction nerve injury; IL33: interleukin-33; ST2: suppressor of tumorigenicity 2; miRNA: microRNA; NC: nonspecific negative control sequence; MWT: mechanical withdrawal threshold; TWL: thermal withdrawal latency.
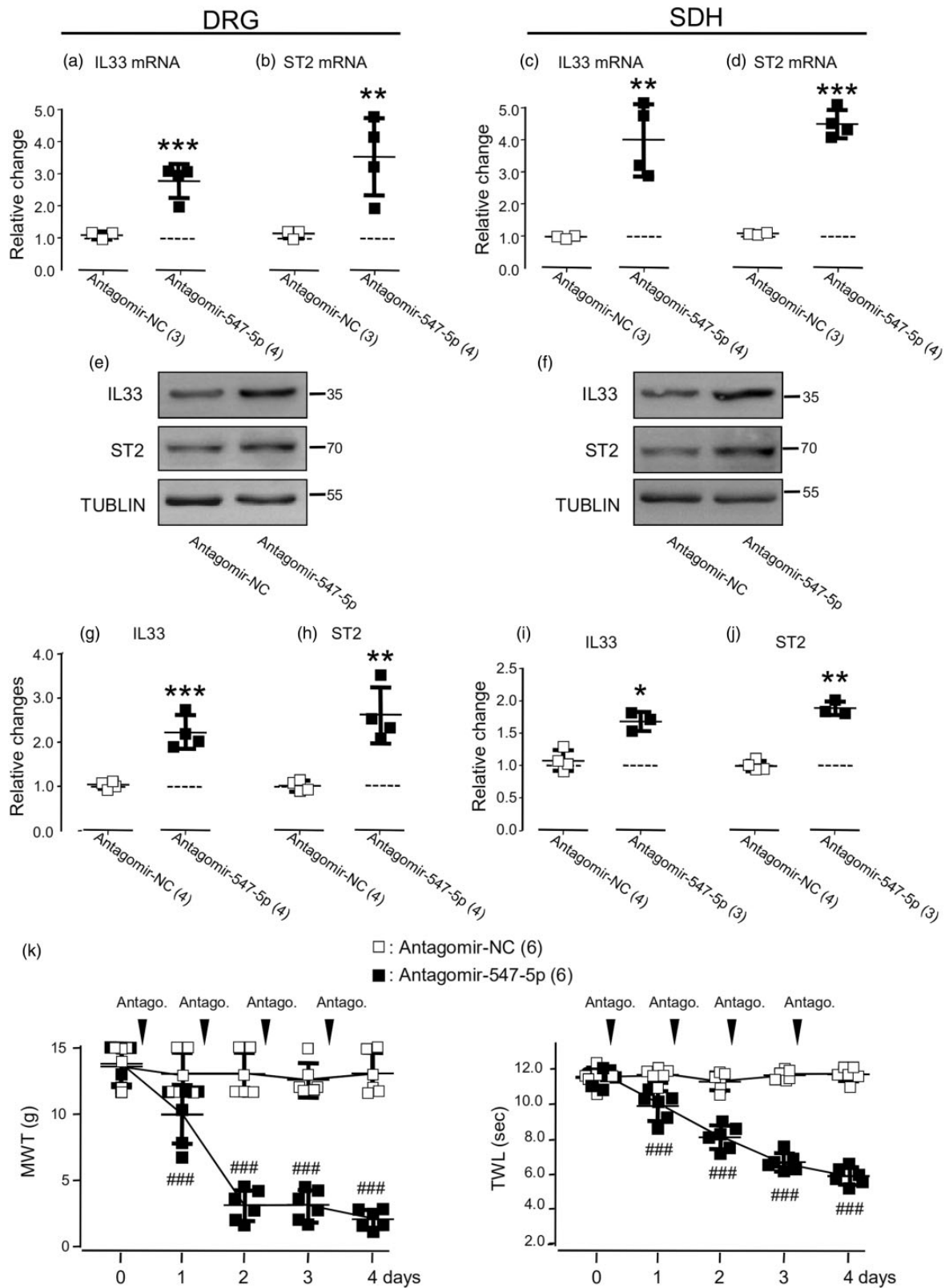
Figure 5. Effects of the i.t. administration of antagomir-miR-547-5p (antagomir-547-5p, 20 μM) on IL-33 (IL33) and ST2. The left graphs of (a) and (c): Summary data (mean ± *SD*) showing the expression of IL-33 mRNA normalized to that in naive rats (= 1, dashed line). The right graphs of (a) and (c): Summary data (mean ± *SD*) showing the expression of IL-33 mRNAs normalized to that in rats that received antagomir-NC (20 μM, = 1, dashed line, see Supplementary Figure 4(a)). The left graphs of (b) and (d): Summary data (mean ± *SD*)

(continued)

study, we examined the effects of BMSC administration on the expression of miR527-5p in the DRG and SDH. When compared to the expression of miR-547-5p in the DRG or SDH of naive rats, no change could be found in rats that received the sham operation or intravenous (i. v.) injection (see Supplementary Figure 5(c)) of BMSCs only (1×10^6 cells in 0.3 ml PBS) (see the left graphs of Figure 7(a) and (b)). However, the CCI-induced reduction in the expression of miR527-5p was reversed by the BMSCs application when compared to that in rats that received the vehicle of BMSCs (see Supplementary Figure 5(d); the right graphs in Figure 7(a) and (b)). Moreover, the increases in IL-33 and ST2 mRNAs or proteins in the DRG or SDH induced by the CCI were also significantly reversed by the BMSC application, which, however, produced no change in the naive rats (see Figure 7).

It has been known that BMSCs may produce analgesic effects by targeting multiple signaling pathways involved in nociceptive functions.[20,35,36] To verify that the modulation of miR-547-5p-mediated IL-33/ST2 pathway is indeed a critical mechanism underlying the analgesic function of BMSCs, we examined effects of the BMSC administration (see Supplementary Figure 5(e)) on antagomir-547-5p-induced changes in the expressions of miR-547-5p, IL-33 and ST2, and the somatosensitivity (see Figure 8). When compared with those in animals only received antagomir-547-5p (see Figure 5(a) to (j)), the BMSC application effectively blocked the increases in the expression of IL-33 and ST2 in both the DRG and SDH induced by delivering antagomir-547-5p (see Figure 8(a) to (f)). Moreover, the BMSC administration (see Supplementary Figure 5(e)) also prevented the antagomir-547-5p delivering-induced decreases in the MWT and TWL (Figure 8(g)). However, when compared to the vehicle application, BMSCs delivered into naive rats did not significantly alter the somatosensitivity

(see Figure 9(a); $p > 0.05$, $F(3, 15) = 0.08$ (MWT); $F(3, 30) = 3.61$ (TWL)).

Consistent with previous findings, the CCI operation significantly reduced the MWT from 14.0 ± 1.4 to 0.8 ± 0.4 g and the TWL from 11.7 ± 0.4 to 4.9 ± 0.2 s (mean $\pm$ SD, n = 6 rats; $p < 0.001$, $F(5, 25) = 429.7$ and 585.2). The BMSC application (see Supplementary Figure 5(f)) significantly reversed the CCI effects: the MWT and TWL were respectively increased by $849.2 \pm 320\%$ and $47 \pm 14\%$ (mean $\pm$ SD, n = 6 rats) (see Figure 9(b)). To determine if altering the miR-547-5p-mediated IL-33/ST2 signaling may be a critical mechanism underlying the analgesic effect of BMSCs on the CCI-induced pain hypersensitivity, we examined the analgesic effects of BMSCs, which were applied into the animals after the treatment with agomir-547-5p (see Supplementary Figure 5(g)) or the sh-IL-33 (see Supplementary Figure 5(h)). We found that the BMSC application conducted after the infusion of agomir-547-5p into animals in the CCI model (see Supplementary Figure 5(g)) only produced $43 \pm 42\%$ and $26 \pm 12\%$ increases in the MWT and TWL. This effect was significantly smaller than those in rats that received BMSC application after infusion of agomir-NC ($p < 0.001$, $t(10) = 17.3$ for MWT; $p < 0.01$, $t(10) = 4.1$ for TWL). BMSC application after the knockdown of IL-33 in CCI-treated animals (see Supplementary Figure 5(h)) produced $17 \pm 8\%$ and $17 \pm 5\%$ increases in MWT and TWL, which were also significantly lower than those in rats that received BMSC application after the infusion of sh-NC (Figure 9(b); $p < 0.001$, $t(10) = 12.8$ for MWT; $p < 0.001$, $t(10) = 12.2$ for TWL). Thus, we concluded that the BMSC effect on the CCI-induced pain hypersensitivity could be occluded by either the miR-547-5p agomir administration or the IL-33 knockdown conducted before the BMSC application.

Figure 5. Continued

showing the expression of ST2 mRNA normalized to that in naive rats (= 1, dashed line). The right graphs in (b) and (d) show the expression of ST2 mRNAs normalized to that in rats that received the i.t. administration of antagomir-NC (= 1, dashed line). (e) and (f) Examples of Western blots. Gels (from left to right) in (e) and (f) were respectively loaded with lysates prepared from the right L4 to L6 DRG (e) and SDH (f) of rats that received the i.t. administration of antagomir-NC and antagomir-547-5p. Each group of the blots was stripped and successively probed with antibodies as indicated on the left of blots. Values on the right side of the blots indicate the molecular mass (Kd). The ratio of band intensities versus that of tublin was calculated. The left graphs in (g) to (j) show normalized ratios to that in naive animals (= 1, dashed line, also see the left blot groups in Figure 4(i) and (j)). The right graphs in (g) to (j) show normalized ratios to that in rats that received the i.t. administration of antagomir-NC (= 1, dashed line). *$p < 0.05$, **$p < 0.01$, ***$p < 0.001$, unpaired t test in comparison between effects of i.t. antagomir-547-5p versus antagomir-NC administration. (k) Summary data (mean $\pm$ SD) showing the effects of the i.t. administration of antagomir-NC (20 μM) or antagomir-547-5p (20 μM) once daily for four consecutive days on the MWT and TWL of rats. The black arrowheads indicate the i.t. infusion of antagomir-NC or antagomir-547-5p. Values in brackets indicate the number of rats tested.

DRG: dorsal root ganglia; SDH: spinal dorsal horn; IL33: interleukin-33; ST2: suppressor of tumorigenicity 2; NC: nonspecific negative control sequence; miRNA: microRNA; MWT: mechanical withdrawal threshold; TWL: thermal withdrawal latency.
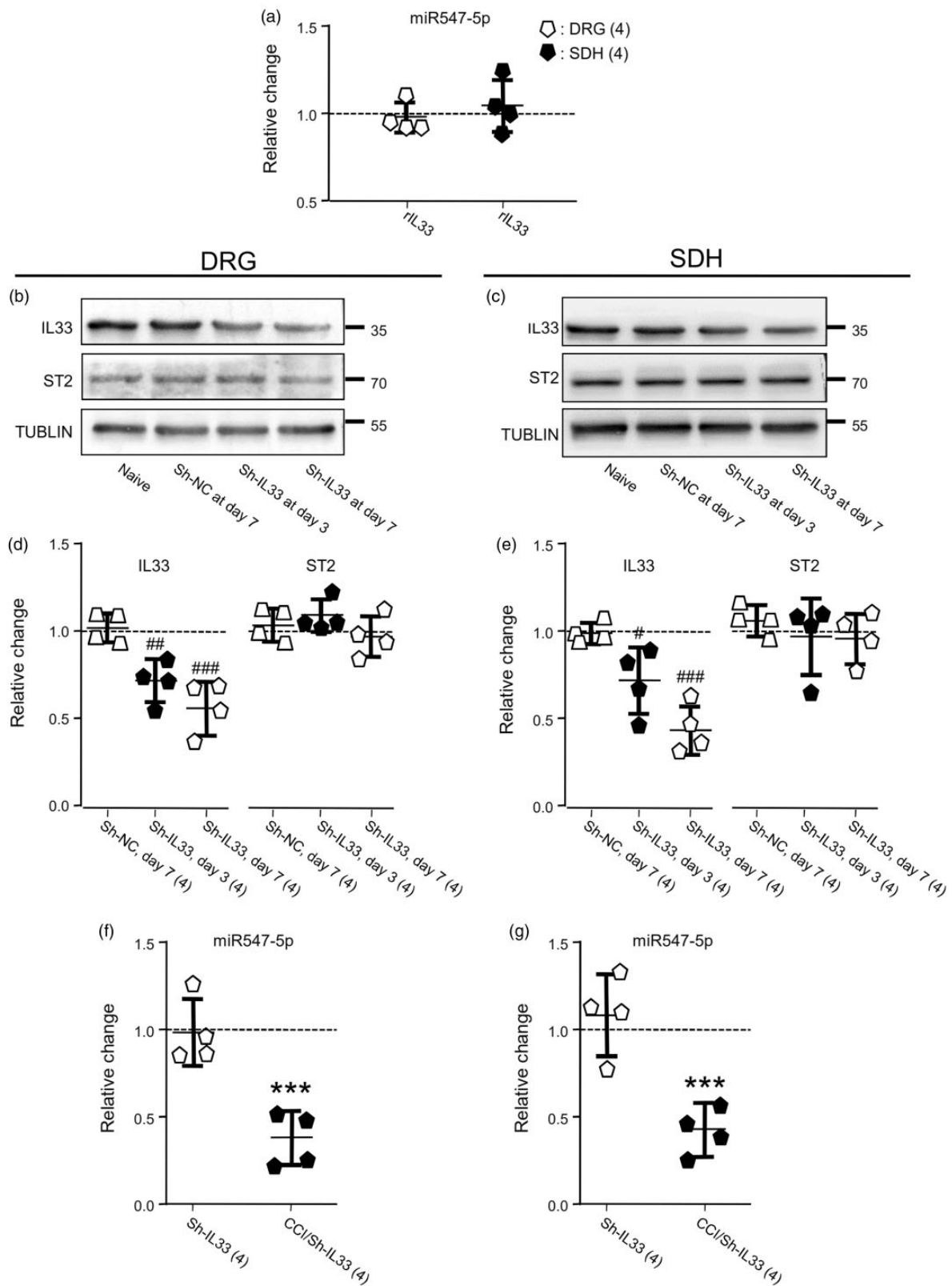
Figure 6. Effects of the i.t. delivering rIL-33 (rIL33) or the knockdown of IL-33 (IL33). (a) Effects of the i.t. delivering rIL-33 (100 ng, Supplementary Figure 5(a)) on the expression of miR547-5p in the DRG and SDH, which were normalized to that in naive rats (= 1, dashed line). (b) and (c) Examples of Western blots. Gels (from left to right) in (b) and (c) were respectively loaded with lysates prepared from the right L4 to L6 DRG (b) and SDH (c) of rats without any treatment (naive), at day 7 after the i.t. infusion of sh-NC (10 μl, Table 1),

(continued)

Furthermore, we did experiments in which agomir-547-5p was applied after the conduction of i.v. treatment with BMSCs into animals in the CCI model (see Supplementary Figure 5(i)). In these animals, the MWT and TWL were 6.53 ± 0.6 g and 7.38 ± 0.45 s right before the agomir-547-5p application and 6.36 ± 0.66 g and 7.27 ± 0.32 s (mean $\pm$ SD, $n = 6$ rats) after the agomir-547-5p application once daily for consecutive 4 days (see Supplementary Figure 5(i)). No significant effect could be found following the agomir-547-5p application (see Figure 9(b)). Thus, the modulation of the miR-547-5p or IL-33/ST2 signaling may be a vital mechanism underlying the anti-nociceptive function of BMSCs (see Figure 9(c)).

Discussion

We found that the expression of the miR-547-5p in both the DRG and SDH ipsilateral to the CCI was significantly decreased and that this miRNA could directly interact with IL-33 and ST2 mRNAs expressed in HEK293T cells. The i.t. administration of agomir-547-5p significantly increased the expression of the endogenous miR-547-5p, whereas its expression was significantly reduced by the i.t. administration of the antagomir-547-5p. Consistent with previous studies,[7,9,10] we found that the expressions of IL-33 and ST2 mRNAs and proteins in the ipsilateral DRG and SDH were significantly increased following the CCI. Agomir-547-5p administration did not produce any significant change in the expression of IL-33 and ST2 and the pain sensitivity in naive rats; however, it blocked the changes in the expression of IL-33 and ST2, and the pain sensitivity in rats with the CCI. These findings strongly suggested a possibility that the reduction of miR-547-5p might be an upstream event leading to the upregulation of IL-33/ST2 signaling following the CCI (see Figure 9(c)).

In contrast to the effects of agomir-547-5p, the i.t. administration of antagomir-547-5p into naive animals not only reduced the expression of endogenous miR-547-5p but also caused increases in the expressions of IL-33 and ST2. In the meantime, pain sensitivity was

significantly increased. This finding provided another line of evidence for that the depressing the miR-547-5p expression could be an upstream signal for the enhancement of the IL-33/ST2 signaling.

Recent studies have shown that IL-33 may dose-dependently induce the proliferation of microglia and enhance the production of pro-inflammatory cytokines, such as IL-1β and tumor necrosis factor-α.[37] Through the extracellular regulated kinase (ERK), p38 mitogen-activated protein kinase (MAPK), c-Jun N-terminal kinase, and nuclear factor-kappa B (NF-κB), IL-33/ST2 signaling exert their functions.[21,38] Via neuronal CaMKII/CREB, NMDA receptor, and astroglial JAK2-STAT3 cascades, the spinal IL-33/ST2 signaling promotes the genesis and maintenance of neuropathic pain.[2,7–9]

Furthermore, it is found that the release of cytokines may be activated in astrocytes following neuropathic injury, which interact with their receptors located on the neuronal surface and thereby causing pain hypersensitivity.[39–41] We found the colocalization of IL-33 and GS or GFAP antibody staining in both the DRG and SDH but no colocalization of IL-33 and NeuN staining (see Supplementary Figures 2 and 3). These data are consistent with previous findings that in the spinal cord, IL-33 is mainly localized in astrocytes.[7,37,42] Similar to those found in the spinal cord and DRG by others,[7,37,42,43] the ST2 was found to be colocalized with NeuN or GFAP staining in the SDH (see Supplementary Figure 3). However, no colocalization of staining with ST2 and GS antibodies was found in the DRG (see Supplementary Figure 2), implying that ST2 in the DRG mainly located in neurons.

Great efforts have been made to clarify mechanisms that may be involved in the regulation of IL-33/ST2 signaling (see reviews: Fairlie-Clarke et al.,[4] Fattori et al.,[10] Molofsky et al.[11]). TNF-α stimulation may increase IL-33 release in isolated mouse pancreatic acinar cells, while IL-33 stimulation may also increase proinflammatory cytokine release; both are involving the ERK/MAPK pathway.[44] It is reported that IL-1β and TNF-α significantly enhance the expression of IL-33 mRNA and

---

Figure 6. Continued

or at day 3 or 7 after the infusion of sh-IL-33 (10 μl, Table 1). (d) and (e) Summary data (mean $\pm$ SD) showing the relative changes in the expression of IL-33 and ST2 proteins in the DRG (d) and SDH (e) normalized with that in naive animals (= 1, dashed line). #$p < 0.05$, ##$p < 0.01$, ###$p < 0.001$ (Dunnett's post hoc test in one-way ANOVA in comparison with that in naive rats). (f) and (g) Summary data (mean $\pm$ SD) showing effects of the IL-33 knockdown on the expression of miR547-5p in the DRG (f) and SDH (g), which were normalized to that in naive rats (= 1, dashed line). sh-IL33: IL-33 was knocked down; CCI/sh-IL33: the CCI was performed in rats on day 7 after the IL-33 knockdown (see Supplementary Figure 5(b)). ***$p < 0.001$, unpaired t test in comparison of the miR547-5p expression after the CCI versus that in naive rats. Values in brackets indicate the number of rats tested.

DRG: dorsal root ganglia; SDH: spinal dorsal horn; IL33: interleukin-33; ST2: suppressor of tumorigenicity 2; CCI: constriction nerve injury; NC: nonspecific negative control sequence.
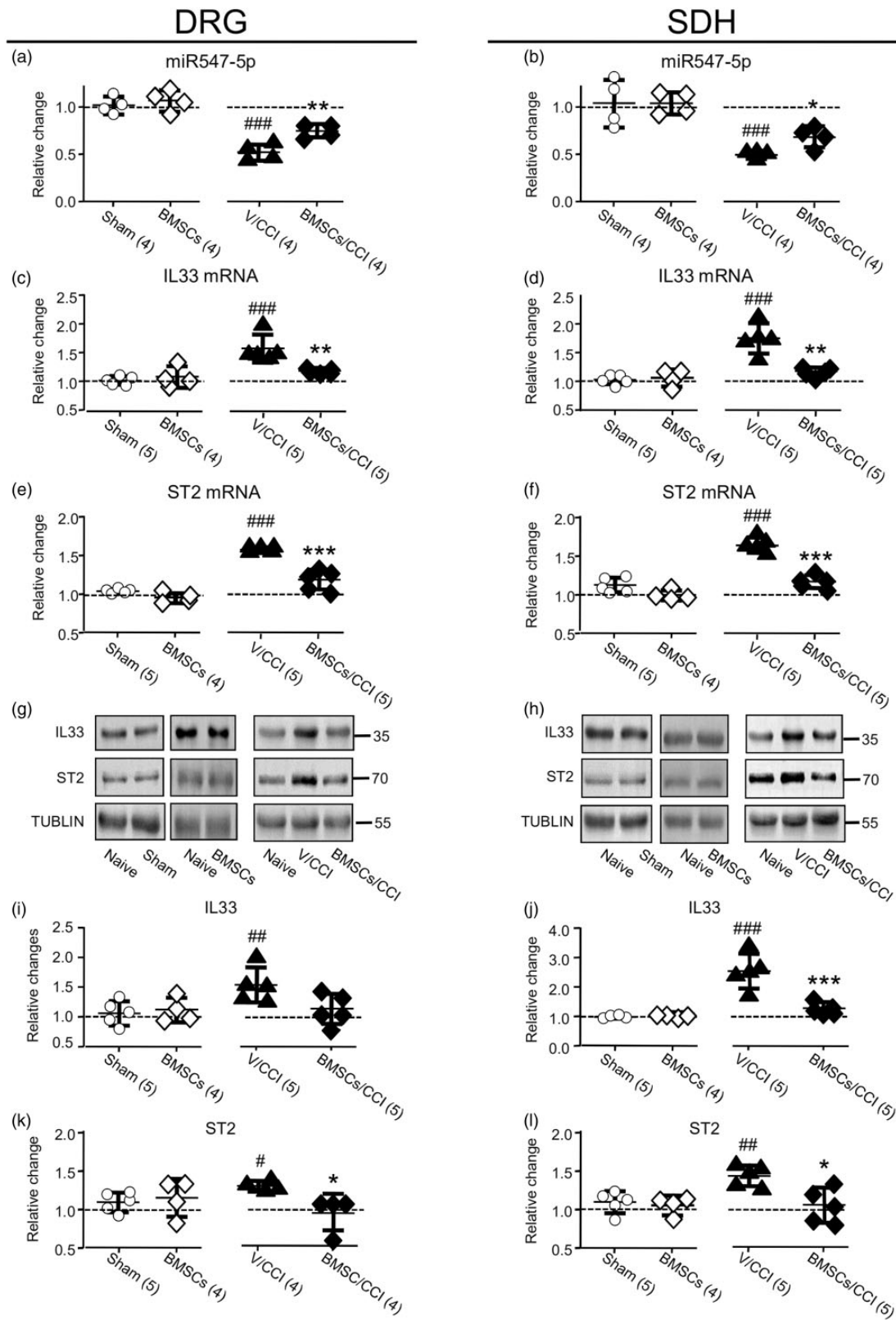
Figure 7. Effects of the BMSC administration on the CCI-induced changes in the expression of miR547-5p, IL-33, or ST2. (a) and (b) Summary data of normalized changes in miR547-5p in the DRG (a) and SDH (b) to that in naive rats (= 1, dashed line). (c) and (d) Summary data of normalized the changes in IL-33 mRNA in the DRG (c) and SDH (d) to that in naive rats (= 1, dashed line). (e) and (f) Summary data of normalized changes in ST2 mRNA in the DRG (e) and SDH (f) to that in naive rats (= 1, dashed line). (g) and (h)

protein in isolated colonic subepithelial myofibroblasts but not in intestinal epithelial cell lines (HT-29 and Caco-2 cells) and that the IL-1β- and TNF-α-induced IL-33 mRNA expression is mediated by p42/44 MAPK pathway-dependent activation of NF-κB and activator protein (AP)-1.[45] However, thus far, the detailed molecular mechanism underlying the enhancement of IL-33/ST2 signaling induced by the CCI remained unclear.

To confirm the possibility that the depression of miR-547-5p might be the upstream event causing the enhancement of IL-33/ST2 signaling induced by the CCI, we investigated the effect of the i.t. infusion of recombinant IL-33, which produced a significant increase in pain sensitivity, on the expression of miR-547-5p. We found that increasing the IL-33 by the i.t. infusion of recombinant IL-33 did not induce any change in the expression of miR-547-5p. Interestingly, the CCI still induced the depression of miR-547-5p expression in the DRG and SDH of rats in which IL-33 was knocked down. This finding excluded the possibility that the depression of miR-547-5p might be induced by the upregulation of IL-33 following the neuropathic stimulation. Taken together, we concluded that the upregulation of IL-33/ST2 signaling, which caused pain hypersensitivity, was a downstream event induced by the depression of miR-547-5p (see Figure 9(c)).

Through regulating neuronal activity, the IRAK1/TRAF6 signaling, or the Nav1.3 channel activity, miRNAs have been found to be involved in the modulation of neuropathic pain induced by nerve injury.[46–50] Enhancing the expression of miRNA-487b may inhibit the expressions of IL-33 and ST2 and prevent the effects produced by IL-33/ST2 signaling.[12,13] It is also found that IL-33/ST2 may promote gut mucosal healing through increasing the expression of miRNA-320 in colitic mice during the recovery period.[14] Although detailed mechanisms underlying the genesis of the depression of miRNA-547-5p by the CCI and the upregulation the IL-33/ST2 signaling by the depression miRNA-547-5p remain to be investigated, the present study has demonstrated that through depressing miRNA-547-5p, the CCI induced the upregulation of the IL-33/ST2 signaling in the DRG and SDH and thereby causing pain hypersensitivity (see Figure 9(c)).

It has been found that BMSCs delivered locally, intrathecally, or systematically may produce a long-lasting analgesic effect (see reviews: Fortino et al.,[15] Huh et al.,[16] Han et al.,[17] Gao and Ji[41]). More detailed studies have shown that the analgesic effect of BMSCs may be achieved through multiple mechanisms, e.g., stimulating immune system,[51] promoting opioid receptors,[20] inhibiting the P2X4 receptor,[52] secreting TGF-β[29] or preventing the release of inflammatory cytokine (such as IL-1β or TNF-α),[30] or inhibiting the γ subtype of protein kinase C and the tyrosine phosphorylation of the GluN2A subunit of N-methyl-D-aspartate receptors.[53]

BMSCs can differentiate to many nonhematopoietic tissues. Many studies have focused on the regulation of stem cells by IL-33/ST2 signaling (see reviews: Fattori et al.,[10] Peine et al.[54]). To date, however, no data reported whether stem cells such as BMSCs might affect the IL-33/ST2 signaling in diseased tissues. Our present study showed that the i.v. application of BMSCs significantly reduced the CCI-induced depression of miR-547-5p, increases in the expression of IL-33 and ST2, and pain hypersensitivity. In contrast, no effect could be found when BMSCs were applied to naive rats.

To determine if altering the miR-547-5p-mediated IL-33/ST2 signaling may be a critical mechanism underlying the analgesic effect of BMSCs on the CCI-induced pain hypersensitivity, we examined the analgesic effects of BMSCs, which were applied to the animals after the treatment with agomir-547-5p or the sh-IL-33. We found that in these animals the analgesic effect produced by BMSC application was significantly reduced when compared with that in animals without the pretreatment or pretreated with agomir-NC or sh-NC. Interestingly, the antagomir-547-5p application performed after the conduction of BMSC treatment could not induce similar changes in pain sensitivity found in animals without the BMSC pretreatment. The agomir-547-5p application performed after the conduction of BMSC treatment in the CCI-model did not produce any significant effect.

Figure 7. Continued
Examples of Western blots. (i) and (j) Summary data of normalized changes in IL-33 protein in the DRG (i) and SDH (j) to that in naive rats (= 1, dashed line). (k) and (l) Summary data of normalized changes in ST2 protein in the DRG (k) and SDH (l) to that in naive rats (= 1, dashed line). Sham: rats with a sham operation; BMSCs: at day 2 after the intravenous (i.v.) infusion of BMSCs (1×10^6 cells in 0.3 ml PBS; see Supplementary Figure 5(c)); V/CCI: the vehicle (0.3 ml PBS) was i.v. administered into rats with CCI (see Supplementary Figure 5(d)); BMSCs/CCI: BMSCs was i.v. administered into rats with CCI (see Supplementary Figure 5(d)). #$p < 0.05$, ##$p < 0.01$, ###$p < 0.001$ (Bonferroni's post hoc test in one-way ANOVA when compared with that in naive rats); *$p < 0.05$, **$p < 0.01$, ***$p < 0.001$ (unpaired t test when compared with that in rats that received the vehicle).
DRG: dorsal root ganglia; SDH: spinal dorsal horn; CCI: constriction nerve injury; BMSC: bone marrow stromal cell; IL33: interleukin-33; miRNA: microRNA; ST2: suppressor of tumorigenicity 2; NC: nonspecific negative control sequence.
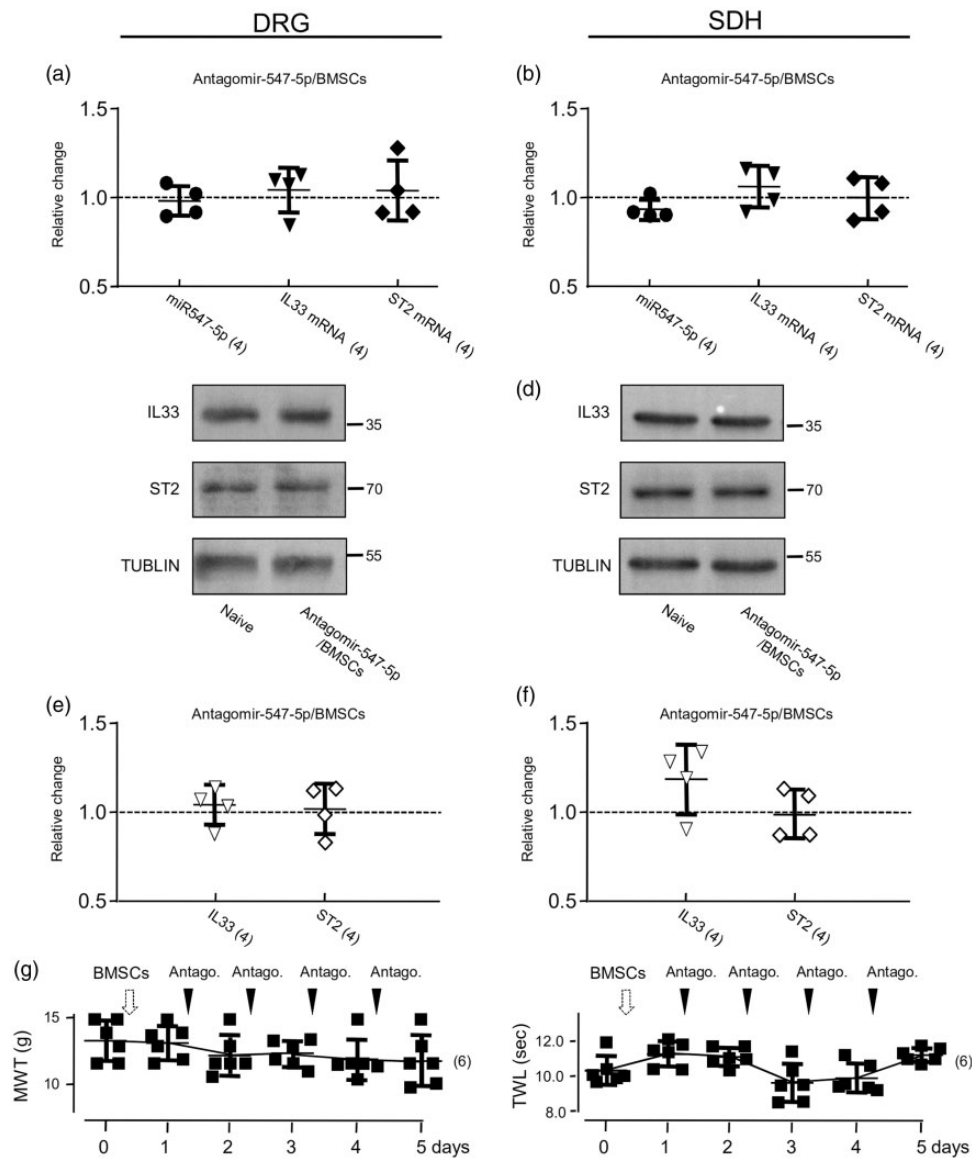
Figure 8. The BMSC administration blocked the effects produced by antagomir-547-5p application. (a) and (b) Summary data of normalized changes in miR547-5p, IL-33 or ST2 mRNAs in the DRG (a) and SDH (b) to that in naive rats (= 1, dashed line). (c) and (d) Examples of Western blots; Antagomir-547-5p/BMSCs: Antagomir-547-5p was i.t. infused into rats pretreated with BMSCs (1×10^6 cells in 0.3 ml PBS). (e) and (f) Summary data of normalized changes in IL-33 and ST2 proteins in the DRG (e) and SDH (f) to that in naive rats (= 1, dashed line). (g) Summary data (mean $\pm$ SD) showing effects of the i.t. administration of antagomir-547-5p (20 μM) on the MWT and TWL of rats pretreated with BMSCs (see Supplementary Figure 5(e)). The black arrowheads indicate the i.t. infusion of antagomir-547-5p. Values in brackets indicate the number of rats tested.

DRG: dorsal root ganglia; SDH: spinal dorsal horn; BMSC: bone marrow stromal cell; IL33: interleukin-33; ST2: suppressor of tumorigenicity 2; MWT: mechanical withdrawal threshold; TWL: thermal withdrawal latency.

Thus, although detailed mechanisms underlying the analgesic effect of BMSCs remained to be clarified, the present findings strongly suggested that BMSCs might produce analgesic effects through targeting the miR-547-5p depression-mediated IL-33/ST2 signaling. However,

understanding the mechanisms underlying BMSC action on miR-547-5p, IL-33, and ST2 still is a challenge, and we still do not know why BMSCs appeared not producing any effect on these molecules in naive animals. These will be essential for further investigations.
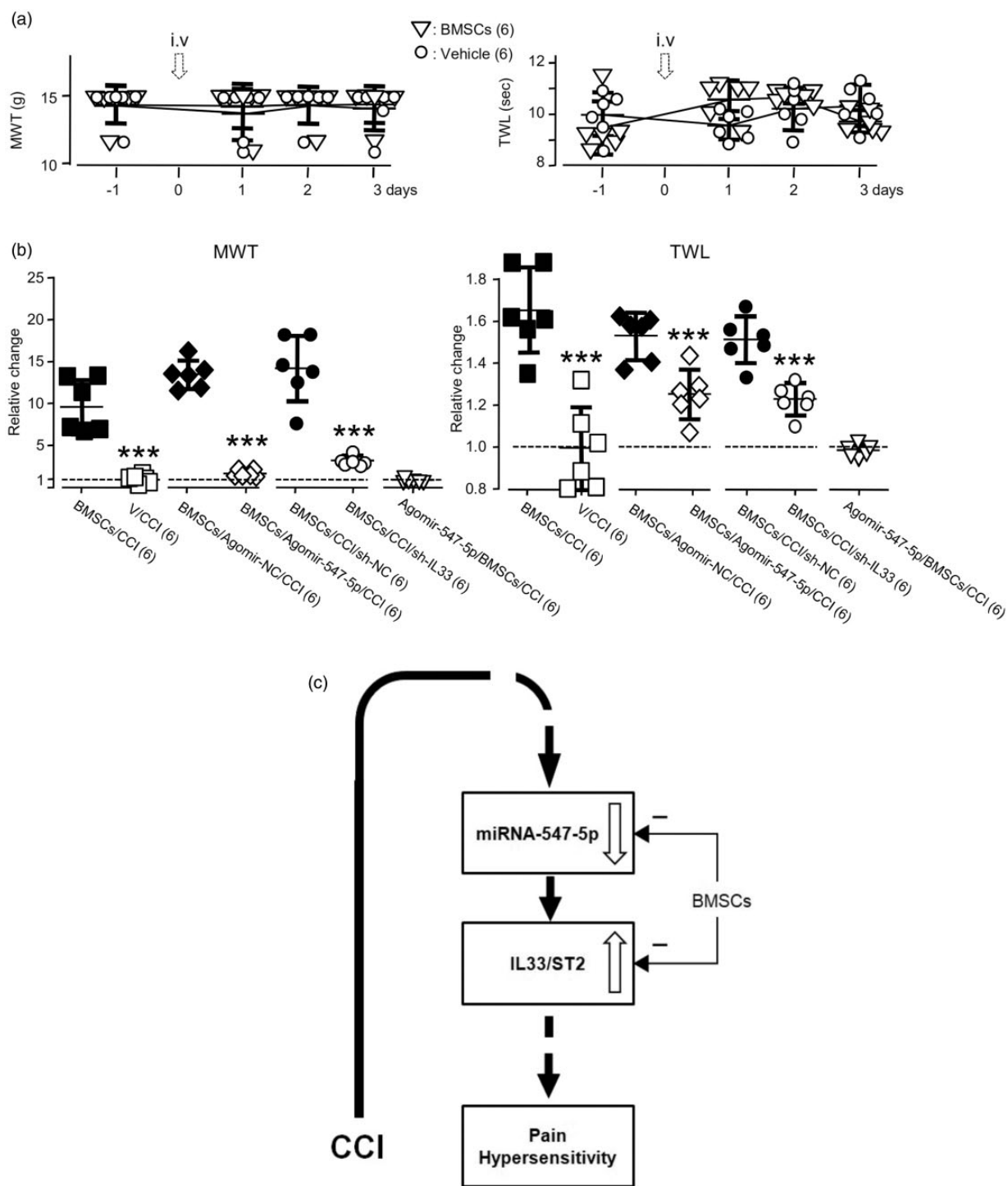
Figure 9. The effects of the administration of agomir-547-5p or the IL-33 knockdown on BMSC administration-induced analgesia in the CCI model. (a) Effects of the i.v. infusion of vehicle or BMSCs on the MWT (left) and TWL (right) in naive rats. (b) Summary data (mean ± *SD*) of normalized changes in the MWT or TWL to that right before the application of the vehicle of BMSCs, BMSCs, Agomir-NC, or Agomir-547-5p (= 1, dashed line). V/CCI: vehicle application in the CCI model (see Supplementary Figure 5(f)); BMSCs/CCI: BMSC application in the CCI model (see Supplementary Figure 5(f)); BMSCs/Agomir-547-5p/CCI: BMSCs were applied after the i.t. administration of agomir-547-5p into rats in the CCI model (see Supplementary Figure 5(g)); BMSCs/Agomir-NC/CCI: BMSCs were applied after the i.t. administration of agomir-NC into rats in the CCI model (see Supplementary Figure 5(g)); BMSCs/sh-IL33/CCI: BMSCs were applied after the i.t. infusion of sh-IL-33 into rats in the CCI model (see Supplementary Figure 5(h)). BMSCs/sh-NC/CCI: BMSCs were applied after the i.t. infusion of sh-NC into rats in the CCI model (see Supplementary Figure 5(h)). Agomir-547-5p/BMSCs/CCI: Agomir-547-5p was applied after the i.v. administration of

Acknowledgments

Author Contributions

Declaration of Conflicting Interests

Funding

ORCID iD

Xian-Min Yu https://orcid.org/0000-0002-9051-6822

References

1. Zarpelon AC, Cunha TM, Alves-Filho JC, Pinto LG, Ferreira SH, McInnes IB, Xu D, Liew FY, Cunha FQ, Verri WA Jr. IL-33/ST2 signalling contributes to carrageenin-induced innate inflammation and inflammatory pain: role of cytokines, endothelin-1 and prostaglandin E2. *Br J Pharmacol* 2013; 169: 90–101.

2. Fattori V, Borghi SM, Verri WA Jr. IL-33/ST2 signaling boosts inflammation and pain. *Proc Natl Acad Sci USA* 2017; 114: E10034–E10035.

3. Du LX, Wang YQ, Hua GQ, Mi WL. IL-33/st2 pathway as a rational therapeutic target for CNS diseases. *Neuroscience* 2018; 369: 222–230.

4. Fairlie-Clarke K, Barbour M, Wilson C, Hridi SU, Allan D, Jiang HR. Expression and function of IL-33/ST2 axis in the central nervous system under normal and diseased conditions. *Front Immunol* 2018; 9: 2596–2512.

5. Alvarez P, Bogen O, Levine JD. Nociceptor interleukin 33 receptor/ST2 signaling in vibration-induced muscle pain in the rat. *J Pain*. Epub ahead of print 25 September 2019. DOI: 10.1016/j.jpain.2019.09.004.

6. Verri WA Jr, Guerrero AT, Fukada SY, Valerio DA, Cunha TM, Xu D, Ferreira SH, Liew FY, Cunha FQ. IL-33 mediates antigen-induced cutaneous and articular hypernociception in mice. *Proc Natl Acad Sci USA* 2008; 105: 2723–2728.

7. Liu S, Mi WL, Li Q, Zhang MT, Han P, Hu S, Mao-Ying QL, Wang YQ. Spinal IL-33/ST2 signaling contributes to neuropathic pain via neuronal CaMKII-CREB and astroglial JAK2-STAT3 cascades in mice. *Anesthesiology* 2015; 123: 1154–1169.

8. Longhi-Balbinot DT, Rossaneis AC, Pinho-Ribeiro FA, Bertozzi MM, Cunha FQ, Alves-Filho JC, Cunha TM, Peron JP, Miranda KM, Casagrande R, Verri WA Jr. The nitroxyl donor, Angeli's salt, reduces chronic constriction injury-induced neuropathic pain. *Chem Biol Interact* 2016; 256: 1–8.

9. Zarpelon AC, Rodrigues FC, Lopes AH, Souza GR, Carvalho TT, Pinto LG, Xu D, Ferreira SH, Alves-Filho JC, McInnes IB, Ryffel B, Quesniaux VF, Reverchon F, Mortaud S, Menuet A, Liew FY, Cunha FQ, Cunha TM, Verri WA Jr. Spinal cord oligodendrocyte-derived alarmin IL-33 mediates neuropathic pain. *Faseb J* 2016; 30: 54–65.

10. Fattori V, Hohmann MSN, Rossaneis AC, Manchope MF, Alves-Filho JC, Cunha TM, Cunha FQ, Verri WA Jr. Targeting IL-33/ST2 signaling: regulation of immune function and analgesia. *Expert Opin Ther Targets* 2017; 21: 1141–1152.

11. Molofsky AB, Savage AK, Locksley RM. Interleukin-33 in tissue homeostasis, injury, and inflammation. *Immunity* 2015; 42: 1005–1019.

12. Wang EW, Jia XS, Ruan CW, Ge ZR. miR-487b mitigates chronic heart failure through inhibition of the IL-33/ST2 signaling pathway. *Oncotarget* 2017; 8: 51688–51702.

13. Liu HC, Liao Y, Liu CQ. miR-487b mitigates allergic rhinitis through inhibition of the IL-33/ST2 signaling pathway. *Eur Rev Med Pharmacol Sci* 2018; 22: 8076–8083.

Figure 9. Continued

BMSCs into rats in the CCI model (see Supplementary Figure 5(i)); ***$p < 0.001$ (unpaired t test in comparison with that of the BMSC application after vehicle, agomir-NC, or sh-NC infusion in the CCI model). Values in brackets indicate the number of rats tested. (c) A diagram shows that via depressing miRNA-547-5p the CCI induces the IL-33/ST2 signaling upregulation and pain hypersensitivity and that via blocking the miRNA-547-5p-mediated IL-33/ST2 signaling, BMSCs reduce the CCI-induced pain hypersensitivity.

BMSC: bone marrow stromal cell; MWT: mechanical withdrawal threshold; TWL: thermal withdrawal latency; IL33: interleukin-33; NC: nonspecific negative control sequence; CCI: constriction nerve injury; ST2: suppressor of tumorigenicity 2; miRNA: microRNA.

14. Lopetuso LR, De Salvo C, Pastorelli L, Rana N, Senkfor HN, Petito V, Di Martino L, Scaldaferri F, Gasbarrini A, Cominelli F, Abbott DW, Goodman WA, Pizarro TT. IL-33 promotes recovery from acute colitis by inducing miR-320 to stimulate epithelial restitution and repair. *Proc Natl Acad Sci USA* 2018; 115: E9362–E9370.

15. Fortino VR, Pelaez D, Cheung HS. Concise review: stem cell therapies for neuropathic pain. *Stem Cells Transl Med* 2013; 2: 394–399.

16. Huh Y, Ji RR, Chen G. Neuroinflammation, bone marrow stem cells, and chronic pain. *Front Immunol* 2017; 8: 1014–1009.

17. Han YH, Kim KH, Abdi S, Kim TK. Stem cell therapy in pain medicine. *Korean J Pain* 2019; 32: 245–255.

18. Bu F, Tian H, Gong S, Zhu Q, Xu GY, Tao J, Jiang X. Phosphorylation of NR2B NMDA subunits by protein kinase C in arcuate nucleus contributes to inflammatory pain in rats. *Sci Rep* 2015; 5: 15945.

19. Ma H, Yao C, Ma P, Zhou J, Gong S, Tao J, Yu XM, Jiang X. Src activation in the hypothalamic arcuate nucleus may play an important role in pain hypersensitivity. *Sci Rep* 2019; 9: 3827–3803.

20. Guo W, Wang H, Zou S, Gu M, Watanabe M, Wei F, Dubner R, Huang GT, Ren K. Bone marrow stromal cells produce long-term pain relief in rat models of persistent pain. *Stem Cells* 2011; 29: 1294–1303.

21. Huang SJ, Yan JQ, Luo H, Zhou LY, Luo JG. IL-33/ST2 signaling contributes to radicular pain by modulating MAPK and NF-kappaB activation and inflammatory mediator expression in the spinal cord in rat models of noncompressive lumber disk herniation. *J Neuroinflammation* 2018; 15: 12.

22. Zielske SP, Stevenson M. Importin 7 may be dispensable for human immunodeficiency virus type 1 and simian immunodeficiency virus infection of primary macrophages. *J Virol* 2005; 79: 11541–11546.

23. Zou J, Zhou Z, Wan L, Tong Y, Qin Y, Wang C, Zhou K. Targeting the sonic hedgehog-gli1 pathway as a potential new therapeutic strategy for myelodysplastic syndromes. *PLoS One* 2015; 10: e0136843.

24. Han Z, Varadharaj S, Giedt RJ, Zweier JL, Szeto HH, Alevriadou BR. Mitochondria-derived reactive oxygen species mediate heme oxygenase-1 expression in sheared endothelial cells. *J Pharmacol Exp Ther* 2009; 329: 94–101.

25. Hou X, Hao X, Zheng M, Xu C, Wang J, Zhou R, Tian Z. CD205-TLR9-IL-12 axis contributes to CpG-induced oversensitive liver injury in HBsAg transgenic mice by promoting the interaction of NKT cells with Kupffer cells. *Cell Mol Immunol* 2017; 14: 675–684.

26. Song C, Wu G, Xiang A, Zhang Q, Li W, Yang G, Shi X, Sun S, Li X. Over-expression of miR-125a-5p inhibits proliferation in C2C12 myoblasts by targeting E2F3. *Acta Biochim Biophys Sin (Shanghai)* 2015; 47: 244–249.

27. He Y, Pan Q, Li J, Chen H, Zhou Q, Hong K, Brugada R, Perez GJ, Brugada P, Chen YH. Kir2.3 knock-down decreases IK1 current in neonatal rat cardiomyocytes. *FEBS Lett* 2008; 582: 2338–2342.

28. Liu S, Zhang P, Chen Z, Liu M, Li X, Tang H. MicroRNA-7 downregulates XIAP expression to suppress cell growth and promote apoptosis in cervical cancer cells. *FEBS Lett* 2013; 587: 2247–2253.

29. Brill AL, Fischer TT, Walters JM, Marlier A, Sewanan LR, Wilson PC, Johnson EK, Moeckel G, Cantley LG, Campbell SG, Nerbonne JM, Chung HJ, Robert ME, Ehrlich BE. Polycystin 2 is increased in disease to protect against stress-induced cell death. *Sci Rep* 2020; 10: 386.

30. Livak KJ, Schmittgen TD. Analysis of relative gene expression data using real-time quantitative PCR and the 2 (-Delta Delta C(T)) method. *Methods* 2001; 25: 402–408.

31. Schmittgen TD, Livak KJ. Analyzing real-time PCR data by the comparative C(T) method. *Nat Protoc* 2008; 3: 1101–1108.

32. Sun XD, Wang A, Ma P, Gong S, Tao J, Yu XM, Jiang X. Regulation of the firing activity by PKA-PKC-Src family kinases in cultured neurons of hypothalamic arcuate nucleus. *J Neurosci Res* 2020; 98: 384–403.

33. Agarwal V, Bell GW, Nam JW, Bartel DP. Predicting effective microRNA target sites in mammalian mRNAs. *Elife* 2015; 4: e05005.

34. Li W, Yin N, Tao W, Wang Q, Fan H, Wang Z. Berberine suppresses IL-33-induced inflammatory responses in mast cells by inactivating NF-kappaB and p38 signaling. *Int Immunopharmacol* 2019; 66: 82–90.

35. Chen G, Park CK, Xie RG, Ji RR. Intrathecal bone marrow stromal cells inhibit neuropathic pain via TGF-beta secretion. *J Clin Invest* 2015; 125: 3226–3240.

36. Ghannam S, Bouffi C, Djouad F, Jorgensen C, Noel D. Immunosuppression by mesenchymal stem cells: mechanisms and clinical applications. *Stem Cell Res Ther* 2010; 1: 2.

37. Yasuoka S, Kawanokuchi J, Parajuli B, Jin S, Doi Y, Noda M, Sonobe Y, Takeuchi H, Mizuno T, Suzumura A. Production and functions of IL-33 in the central nervous system. *Brain Res* 2011; 1385: 8–17.

38. Schmitz J, Owyang A, Oldham E, Song Y, Murphy E, McClanahan TK, Zurawski G, Moshrefi M, Qin J, Li X, Gorman DM, Bazan JF, Kastelein RA. IL-33, an interleukin-1-like cytokine that signals via the IL-1 receptor-related protein ST2 and induces T helper type 2-associated cytokines. *Immunity* 2005; 23: 479–490.

39. Chiang CY, Wang J, Xie YF, Zhang S, Hu JW, Dostrovsky JO, Sessle BJ. Astroglial glutamate-glutamine shuttle is involved in central sensitization of nociceptive neurons in rat medullary dorsal horn. *J Neurosci* 2007; 27: 9068–9076.

40. Kawasaki Y, Zhang L, Cheng JK, Ji RR. Cytokine mechanisms of central sensitization: distinct and overlapping role of interleukin-1beta, interleukin-6, and tumor necrosis factor-alpha in regulating synaptic and neuronal activity in the superficial spinal cord. *J Neurosci* 2008; 28: 5189–5194.

41. Gao YJ, Ji RR. Chemokines, neuronal-glial interactions, and central processing of neuropathic pain. *Pharmacol Ther* 2010; 126: 56–68.

42. Zhao J, Zhang H, Liu SB, Han P, Hu S, Li Q, Wang ZF, Mao-Ying QL, Chen HM, Jiang JW, Wu GC, Mi WL, Wang YQ. Spinal interleukin-33 and its receptor ST2 contribute to bone cancer-induced pain in mice. *Neuroscience* 2013; 253: 172–182.

43. Liu B, Tai Y, Achanta S, Kaelberer MM, Caceres AI, Shao X, Fang J, Jordt SE. IL-33/ST2 signaling excites sensory neurons and mediates itch response in a mouse model of poison ivy contact allergy. *Proc Natl Acad Sci USA* 2016; 113: E7572–E7579.

44. Kempuraj D, Twait EC, Williard DE, Yuan Z, Meyerholz DK, Samuel I. The novel cytokine interleukin-33 activates acinar cell proinflammatory pathways and induces acute pancreatic inflammation in mice. *PLoS One* 2013; 8: e56866.

45. Kobori A, Yagi Y, Imaeda H, Ban H, Bamba S, Tsujikawa T, Saito Y, Fujiyama Y, Andoh A. Interleukin-33 expression is specifically enhanced in inflamed mucosa of ulcerative colitis. *J Gastroenterol* 2010; 45: 999–1007.

46. Bai G, Ren K, Dubner R. Epigenetic regulation of persistent pain. *Transl Res* 2015; 165: 177–199.

47. Sakai A, Saitow F, Miyake N, Miyake K, Shimada T, Suzuki H. miR-7a alleviates the maintenance of neuropathic pain through regulation of neuronal excitability. *Brain* 2013; 136: 2738–2750.

48. Su S, Shao J, Zhao Q, Ren X, Cai W, Li L, Bai Q, Chen X, Xu B, Wang J, Cao J, Zang W. MiR-30b attenuates neuropathic pain by regulating voltage-gated sodium channel Nav1.3 in rats. *Front Mol Neurosci* 2017; 10: 126–105.

49. Wang Z, Liu F, Wei M, Qiu Y, Ma C, Shen L, Huang Y. Chronic constriction injury-induced microRNA-146a-5p alleviates neuropathic pain through suppression of IRAK1/TRAF6 signaling pathway. *J Neuroinflammation* 2018; 15: 179–106.

50. Malcangio M. Role of the immune system in neuropathic pain. *Scand J Pain* 2019; 20: 33–37.

51. Guo W, Imai S, Yang JL, Zou S, Watanabe M, Chu YX, Mohammad Z, Xu H, Moudgil KD, Wei F, Dubner R, Ren K. In vivo immune interactions of multipotent stromal cells underlie their long-lasting pain-relieving effect. *Sci Rep* 2017; 7: 10107.

52. Teng Y, Zhang Y, Yue S, Chen H, Qu Y, Wei H, Jia X. Intrathecal injection of bone marrow stromal cells attenuates neuropathic pain via inhibition of P2X4R in spinal cord microglia. *J Neuroinflammation* 2019; 16: 271.

53. Guo W, Chu YX, Imai S, Yang JL, Zou S, Mohammad Z, Wei F, Dubner R, Ren K. Further observations on the behavioral and neural effects of bone marrow stromal cells in rodent pain models. *Mol Pain* 2016; 12: 174480691665804.

54. Peine M, Marek RM, Lohning M. IL-33 in T cell differentiation, function, and immune homeostasis. *Trends Immunol* 2016; 37: 321–333.